



Mean Diurnal Patterns for Select Stations in the TOGA COARE Region

Julie Caron, Shawn Smith, David Legler

Center for Ocean-Atmospheric Prediction Studies
Surface Meteorology Data Processing Center
COARE Report 96-2
August, 1996

Acknowledgements: Discussions with individuals in the Center for Ocean-Atmospheric Prediction Studies (COAPS) improved the scope and content of this atlas. A special thank you to Mark Verschell and James Stricherz for sharing their computing expertise.

We acknowledge support from NOAA/UCAR through the TOGA COARE International Project Office (Contract S94-39979).

1. Introduction

The main objective of the atlas is to provide insight into the mean diurnal patterns of surface meteorology variables during the Tropical Ocean Global Atmosphere Coupled Ocean Atmosphere Response Experiment (TOGA COARE). The geographical region considered for this atlas is bounded by 30S to 30N and 180E to 90E (see Fig. 1). The mean diurnal patterns for 37 land stations in this region are presented. They were calculated based on data available every three hours (where possible), during the Intensive Observing Period (IOP): 00UTC on November 1, 1992 to 23UTC on February 28, 1993.

Early atlases of the TOGA COARE region provide (monthly and 20 year) climatological isoline and streamline analyses of kinematic and thermodynamic meteorological parameters. For example, they provide monthly and 15 year climatological analyses of in-situ wind data over the Indian Ocean (Ref2); similarly for the Tropical Pacific (Ref3). Moreover, model analyses of surface meteorological parameters and their anomalies provide a climatology of the TOGA COARE Region (1985-1990)(Ref4). Specific attention is given to the IOP (4 month) climatology throughout.

The advantage of diurnal diagrams is that they efficiently highlight sea and land breeze patterns, surface pressure tidal signatures, and other localized patterns. In the tropics we expect that the dynamics will be dominated by meso-scale events, and thus will occur on shorter time scales than in the middle latitudes (Ref1). This atlas provides mean diurnal diagrams of wind speed and direction, air temperature, atmospheric pressure, specific humidity, and normalized specific humidity. The normalized specific humidity is a ratio of the specific humidity to the saturation specific humidity, reported in units of percent.

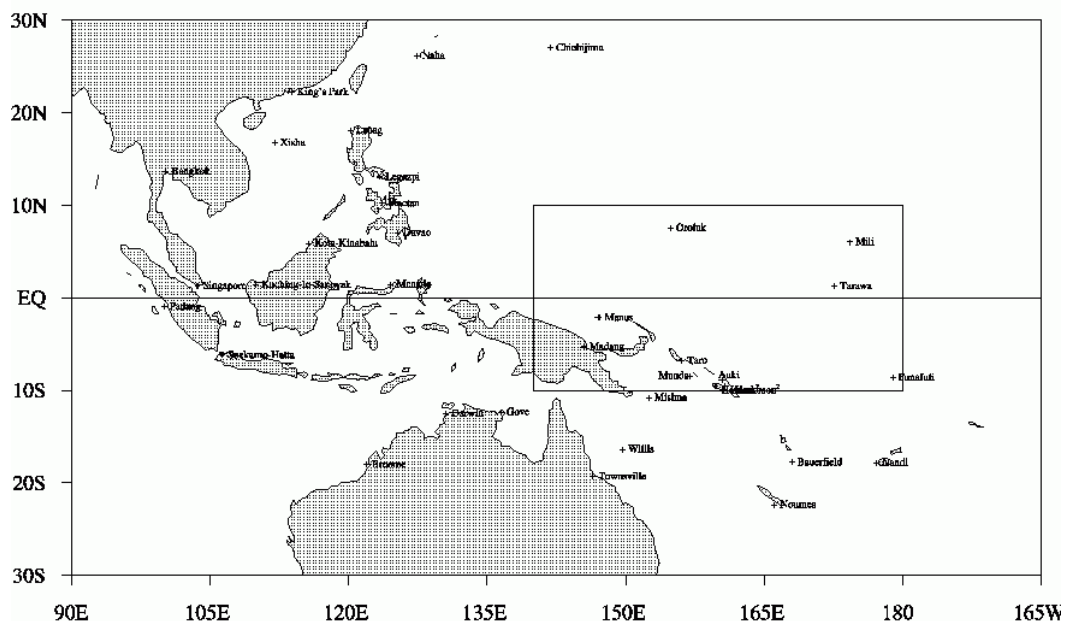


Fig.1: Land stations selected for this atlas.

2. Data

The data for these analyses were obtained from the Data Services Section of the National Center for Atmospheric Research (NCAR), and consist of data transmitted via the Global Telecommunications System (GTS) and the Integrated Sounding Systems (ISS) during the TOGA COARE IOP. All land station data were quality controlled by the Surface Meteorology Data Processing Center at the Florida State University, (hereafter referred to as COAREMET). The COAREMET quality control process contained two steps. Initially, an automated low-level scan determined coding errors, spurious spikes, instrument drift or failure, and unrealistic data. These data were then inspected visually, and an appropriate pass or fail flag was assigned. Second, comparisons between the data across platforms and instruments, were made and any discrepancies noted.

After quality control, the stations chosen for this analysis were based on two criteria. The first requires that the data record for the station have a minimum of 480 of the possible 960 three-hourly records. The value of 960 represents the count of three hourly data taken daily during the entire IOP. Further, the first criterion was applied to only those data which are considered good via FSU DPC quality-control. Only three of the sixteen possible quality-control flags are considered acceptable. Observations flagged as correct, containing an interesting feature, and/or those data that originally had unknown units, but which have since been determined by FSU DPC are all accepted for analysis.

The second criterion requires that there be at least four uniformly distributed observations per day for at least one half of the 120 possible days of data. For example, a diurnal cycle could be derived from observations every six hours, if at least half of the 120-day time period entries for any one observation time consist of acceptable data (i.e. Table 1).

HOUR (UTC)	Bauerfield Pressure Records	Bauerfield Temperature Records	Cocos Pressure Records	Cocos Temperature Records
0	120	120	119	119
3	104	105	112	112
6	117	118	120	120
9	106	106	62	63
12	117	117	70	70
15	110	111	1	1
18	118	117	1	19
21	109	109	16	15

Table 1: An example of pressure and temperature records for two land stations (Bauerfield and Cocos). Bauerfield meets criteria number two; Cocos does not.

The first criterion eliminated 39 (51%) of the original 79 land stations for which we had GTS or ISS data. The second criterion eliminated three more stations, leaving 37 stations for the analysis (Fig. 1).

Some stations were included that had special stipulations regarding the temperature, pressure, specific humidity, and normalized specific humidity data. Misima, Soekarno-Hatta, and Taro were analyzed at six hour intervals, beginning with 00UTC, since those were the only times which met all the criteria. Funafuti, Momote, and Broome will be evaluated every three hours except 15UTC (due to insufficient data at that observation time). Auki and Honiara will be evaluated every six hours, except the 21UTC observation will be used in lieu of the less plentiful 18UTC observation. For both Oroluk and Mili, only the temperature and pressure diurnal cycles will be analyzed, as not enough data remained for the other parameters.

The above criteria also applied to the wind data. As a result, Funafuti, Momote, and Misima have insufficient wind observations at 15UTC, and thus are evaluated for the remaining three hourly observation times only. Moreover, winds were not analyzed for Padang, Mili, Menado, Madang, Taro, Auki, and Honiara due to a lack of wind data. Winds were not analyzed for Munda, because these data did not meet criterion two.

For stations that reported calm winds, the wind direction was ignored, since a wind direction in that case would have no meaning. Moreover, in the cases where no wind direction data existed, the wind speeds were also ignored.

3. About The Atlas

Part I:

This atlas contains temperature, pressure, specific humidity, and normalized specific humidity diurnal plots for those land stations which met all the required criteria. In each figure, the diurnal cycles are displayed with solid lines and the dashed lines represent the standard error.

The diurnal cycles were produced by calculating averages of the data at each observation time over the entire 120 days. Further, the standard error for each parameter was given by

$$se = s / \sqrt{N} \quad (1)$$

where s is the standard deviation and N represents the number of observations at each observation time. These were plotted as a range about the observed mean diurnal cycle, for the temperature, pressure, specific humidity, and normalized specific humidity.

Part II:

This atlas also contains wind roses computed at each selected observation time hours (where possible) which categorize each land station's wind direction and magnitude on a sixteen point compass (Table 2). Following the meteorological convention, the compass orientation

represents the direction from which the wind is coming. A direction ratio was computed every three hours. It is defined as the number of times the wind direction falls in a particular direction range to the number of good observations for that observation time. The axes of the wind rose represent these direction ratios in units of percent. The winds speeds are divided into nine categories (Table 3). Each wind speed category corresponds to a different line thickness on the wind rose.

CATEGORY	RANGE(degrees)	DIRECTION
1	348 to 12	N
2	12 to 33	NNE
3	33 to 56	NE
4	56 to 78	ENE
5	78 to 101	E
6	101 to 123	ESE
7	123 to 146	SE
8	146 to 168	SSE
9	168 to 191	S
10	191 ro 213	SSW
11	213 to 236	SW
12	236 to 258	WSW
13	258 to 281	W
14	281 to 303	WNW
15	303 to 326	NW
16	326 to 348	NNW

Table 2: Listed here are the sixteen wind direction categories, their corresponding ranges and directions.

CATEGORY	SPEED
1	1-2 knots
2	2-3 knots
3	3-4 knots
4	4-5 knots
5	5-6 knots
6	6-7 knots
7	7-10 knots
8	10-15knots
9	15+ knots

Table 3: Nine wind speed categories which correspond to wind rose magnitudes.

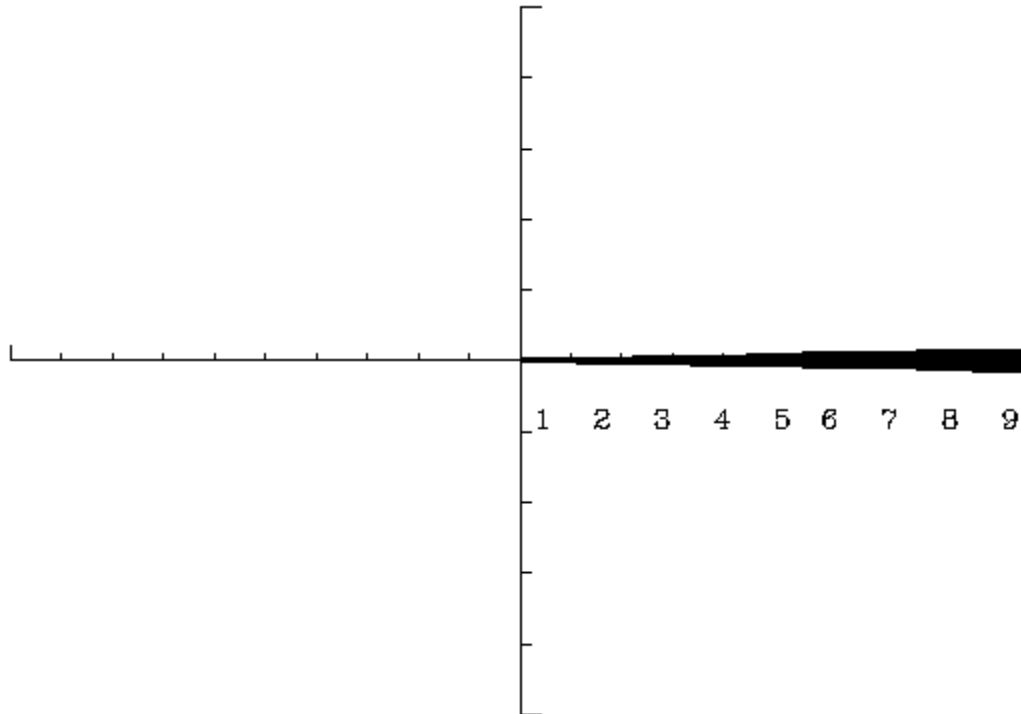


Fig. 2: Wind rose legend illustrating the nine wind speed categories, corresponding to line thicknesses.

4. Interpretation:

The diurnal cycles for atmospheric pressure, air temperature, specific humidity, and normalized specific humidity contain very similar patterns for each of the land stations in close proximity. In all the mean diurnal pressure patterns, the solar semi-diurnal tidal signature is clearly evident (Ref1). We expect that the amplitude of this 12-hourly pressure oscillation would have a maximum near the equator and would decrease poleward. We found, however, that the amplitude is approximately 2mb, for this region, with no obvious poleward decrease. The minima occur between 4 and 6UTC and between 15 and 18UTC, while the maxima occur between 10 and 13UTC and between 21 and 3UTC. It is clearly evident that the propagation of these tidal waves is from East to West. For example, the first minimum occurs on average approximately 3z at Funafuti, while it occurs at 6UTC in Taro and at 9UTC in Kuching. Daily variations in air temperature in this region are approximately 4 degrees Celsius. As expected, the daily air temperature maximum occurs between 03 and 05 UTC, corresponding to the afternoon, while the minimum occurs around 16 or 18 UTC. The daily specific humidity patterns for most stations tend to resemble the diurnal air temperature patterns, especially for land stations on small islands. The stations at higher latitudes, such as Noumea and Chichijima, exhibit higher variability in the the diurnal patterns of specific humidity. Stations very close to the equator, such as Singapore and Kuching-In-Sarawak, have a diurnal specific humidity pattern which resembles the tidal pressure pattern.

Upon comparison of the wind roses, the resulting mean winds appear to follow the long-term climatological patterns, as illustrated in Stricherz, et. al. (Refs 2,3). The land stations, such as Oroluk and Legazpi which are located near ten degrees north of the equator, have prevailing NE and E wind directions, which reflect the seasonal change in wind direction during the northern hemisphere winter, associated with the southward migration of the ITCZ. In most cases, the seasonal climatological signal tends to dominate the wind patterns leaving the occurrences of diurnal wind variations indiscernible. This signal is characterized by light and variable winds between 10N and 10S during November. Near 10N, there is a strengthening Northerly/Northeasterly component through December, January, and February. This Northerly component tends to dominate from the equator to 10N.

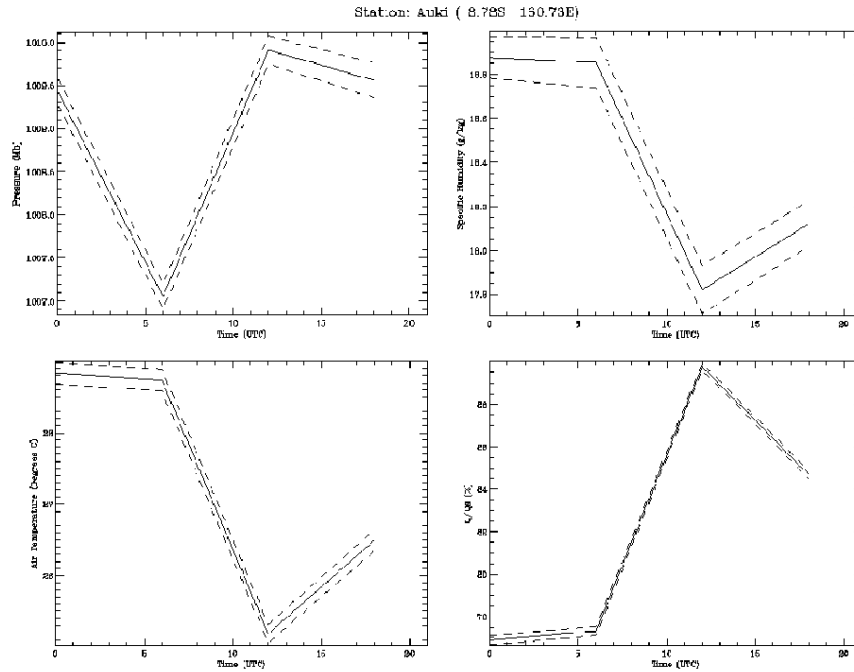
For some portions of the region surrounding TOGA COARE LSA latitudes higher than 10 degrees), the climatological winds are not as pronounced in magnitude and thus it is possible that the flow regimes for these stations are dominated by localized topographic effects. Darwin for example, has strong westerly onshore flow while any easterly flow is blocked, because it is located on the windward side of the hilly Arnhem Land in Northern Australia. Gove; however, is located further east than Darwin, and has more variable wind directions due to the effect of the nearby hills and valleys.

5. Conclusion:

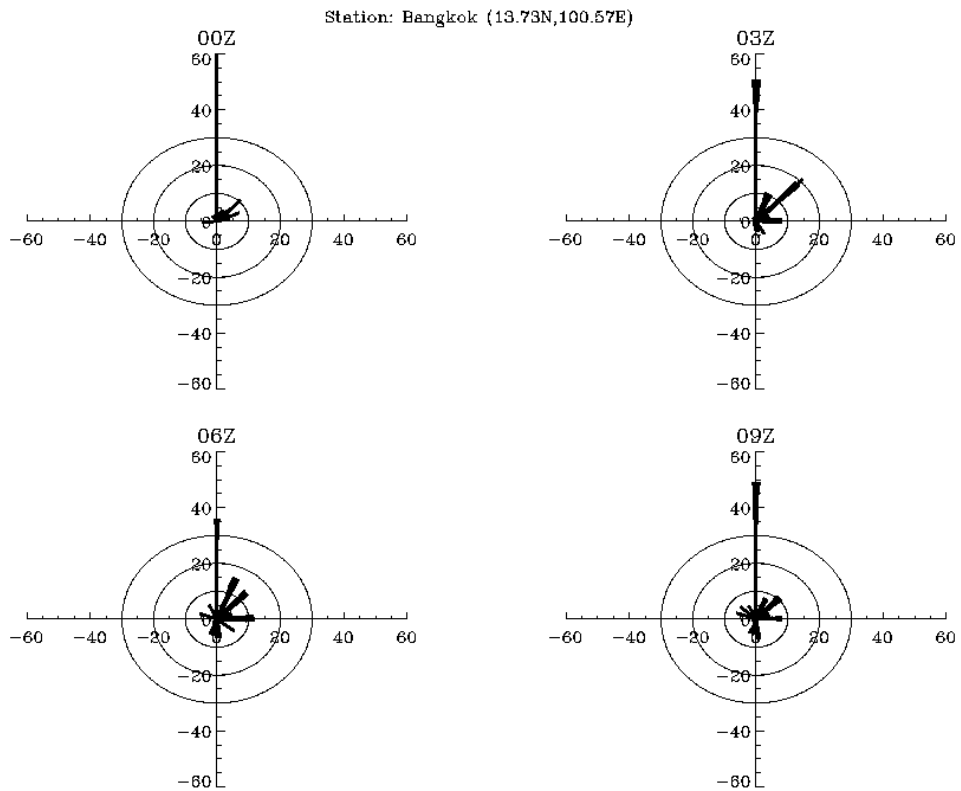
Analysis of climatological patterns that occur on time scales of a day can aid in our understanding of the surface meteorology of the TOGA COARE region. This region exhibits a tidal signature in the mean semi-diurnal atmospheric pressure pattern at most stations. Further, the stations located on small islands show clear correlation with seasonal climatological wind directions over the Pacific and Indian Oceans; however, they do not seem to yield clear insight into strong diurnal wind variations such as sea and land breezes. The diurnal specific humidity patterns were found to be affected by the pressure tidal pattern near the equator and by the temperature pattern at higher latitudes.

6. REFERENCES

- 1. Climate Dynamics of the Tropics**, Stefan Hastenrath, Kluwer Academic Publishers, 1991.
- 2. Atlas of Florida State University Indian Ocean Winds for TOGA 1970-1985**, James N. Stricherz, David M. Legler, and James J. O'Brien, Florida State University, Mesoscale Air-Sea Interaction Group Technical Report, Aug. 1993.
- Atlas of Florida State University Tropical Pacific Winds for TOGA 1966- 1985**, James N. Stricherz, James J. O'Brien, and David M. Legler, Florida State University, Mesoscale Air-Sea Interaction Group Technical Report, Aug., 1992.
- 4. Climatology of the TOGA - COARE and Adjacent Regions (1985-1990)**, Dayton G. Vincent and Jon M. Schrage, Purdue University, Department of Earth and Atmospheric Sciences, Dec., 1995.

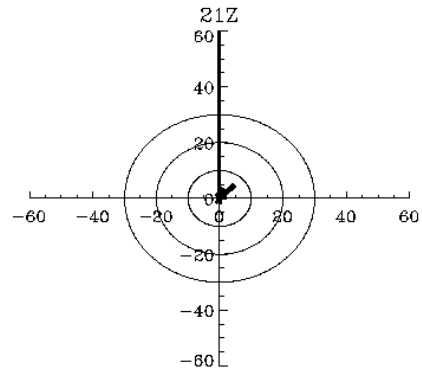
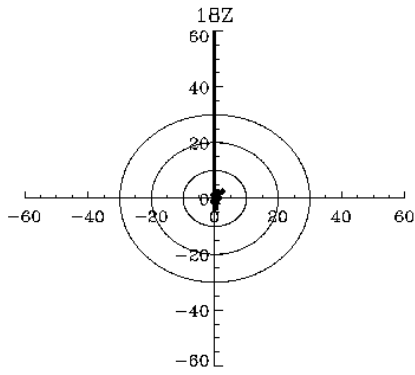
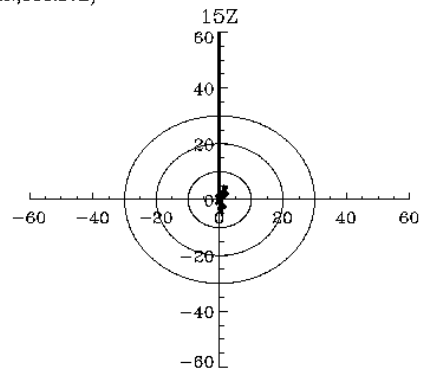
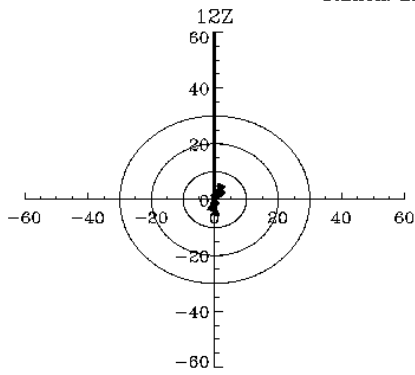


Station Auki (91507) diurnal changes



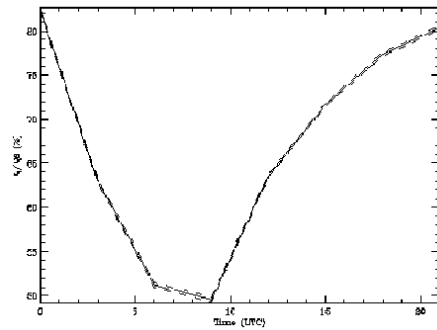
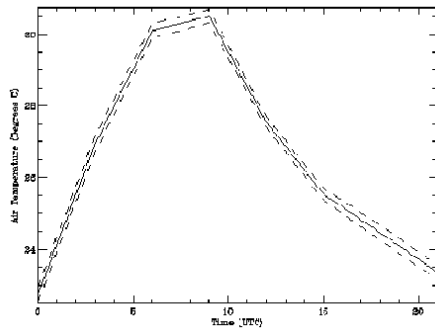
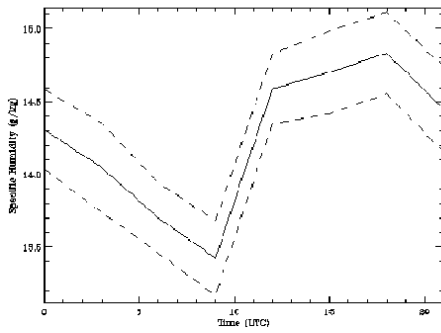
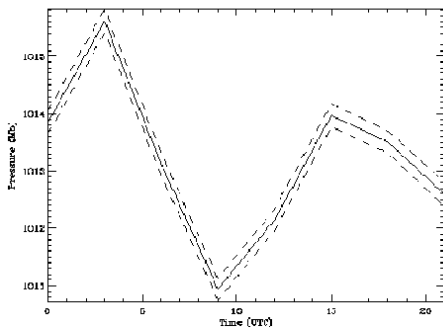
Station Bangkok (48455) 0,3,6,9 UTC Wind Roses

Station: Bangkok (13.73N,100.57E)



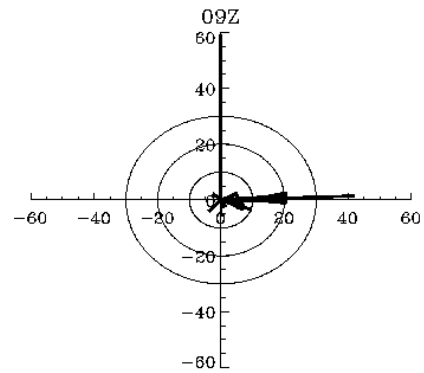
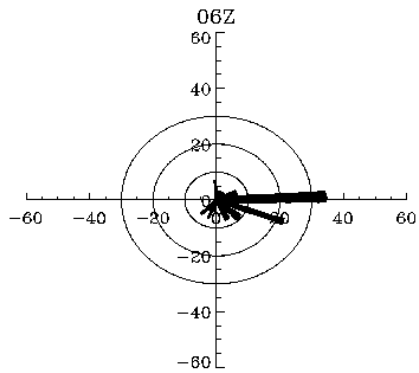
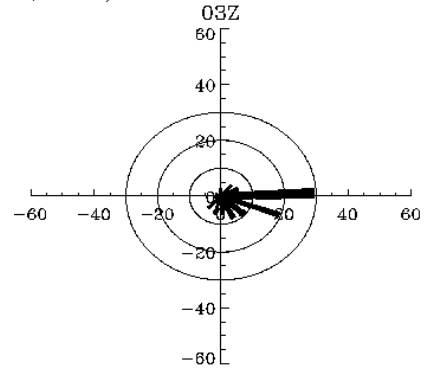
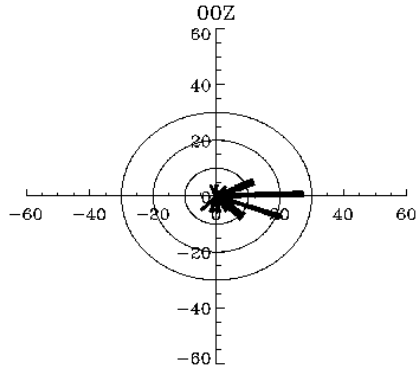
Station Bangkok (48455) 12,15,18,21 UTC Wind Roses

Station: Bangkok (13.73N 100.57E)



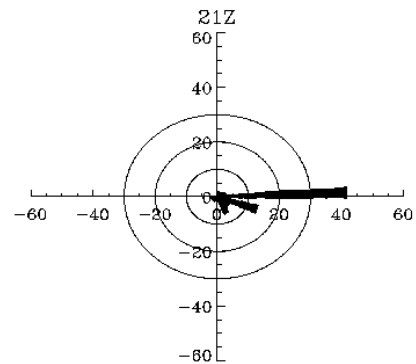
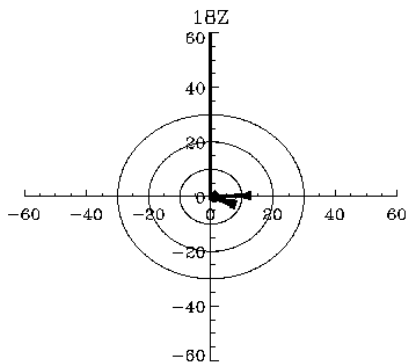
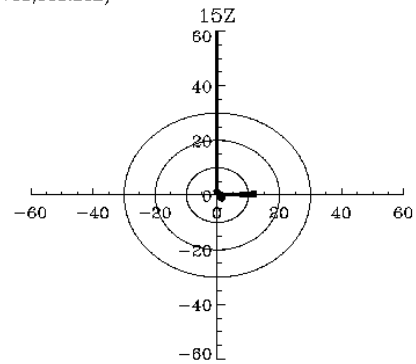
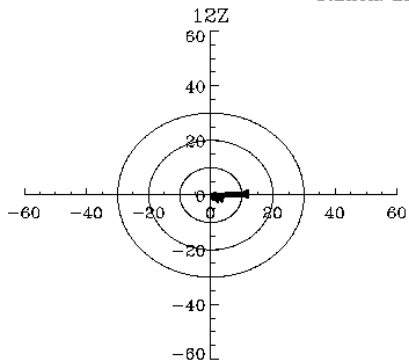
Station Bangkok (48455) diurnal changes

Station: Bauerfield (17.70S,168.30E)



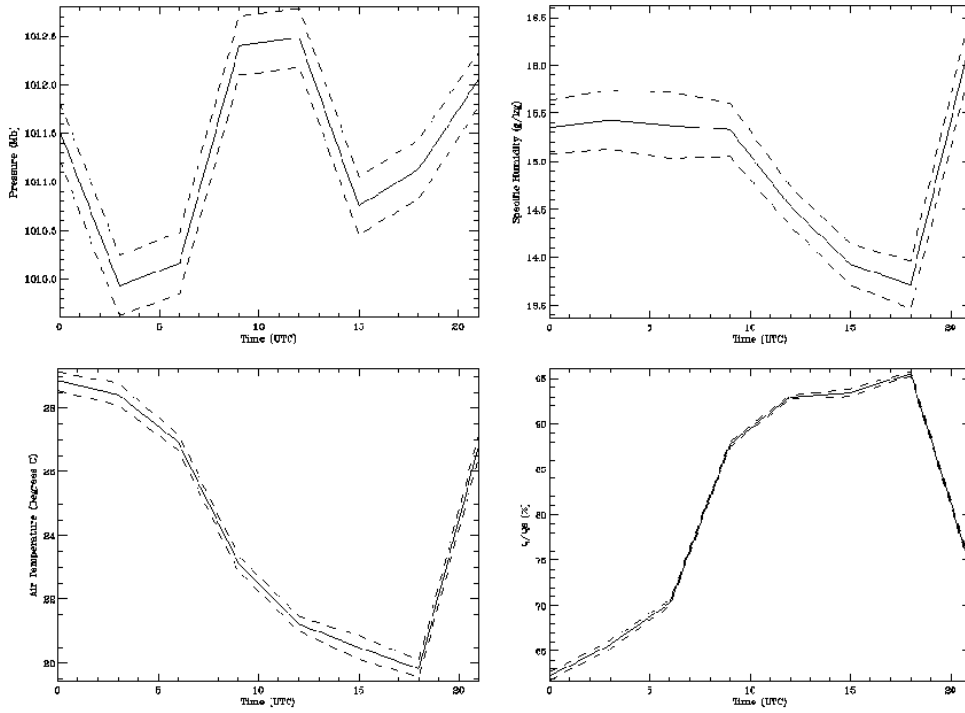
Station Bauerfield (91557) 0,3,6,9 UTC Wind Roses

Station: Bauerfield (17.70S,168.30E)



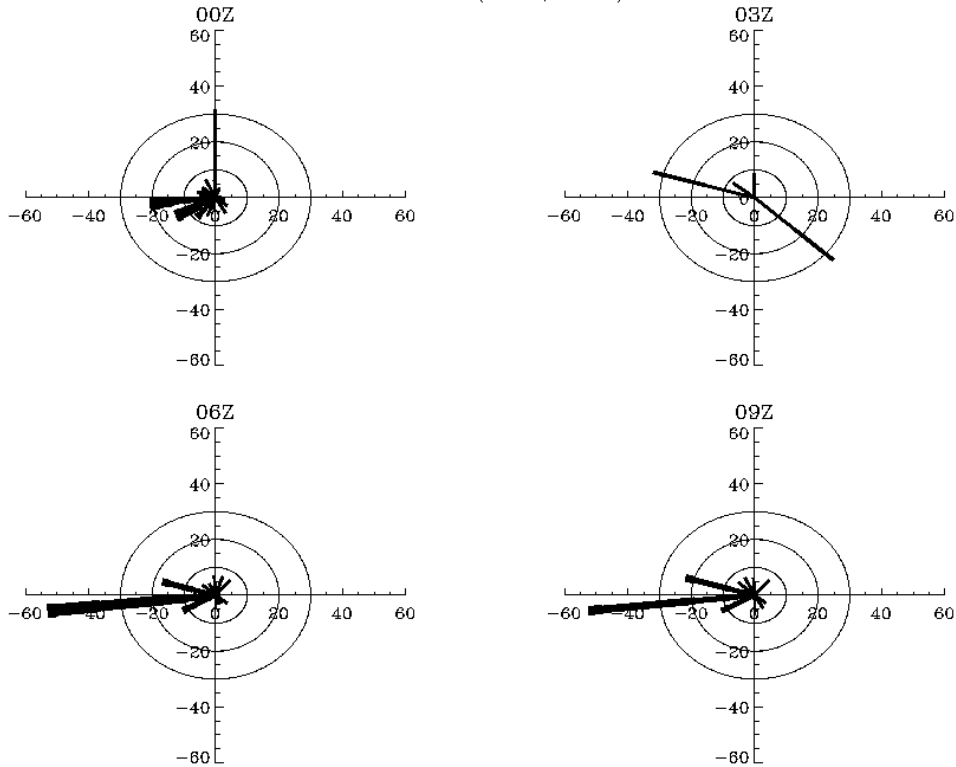
Station Bauerfield (91557) 12,15,18,21 UTC Wind Roses

Station: Bauerfield (17.70S 168.30E)



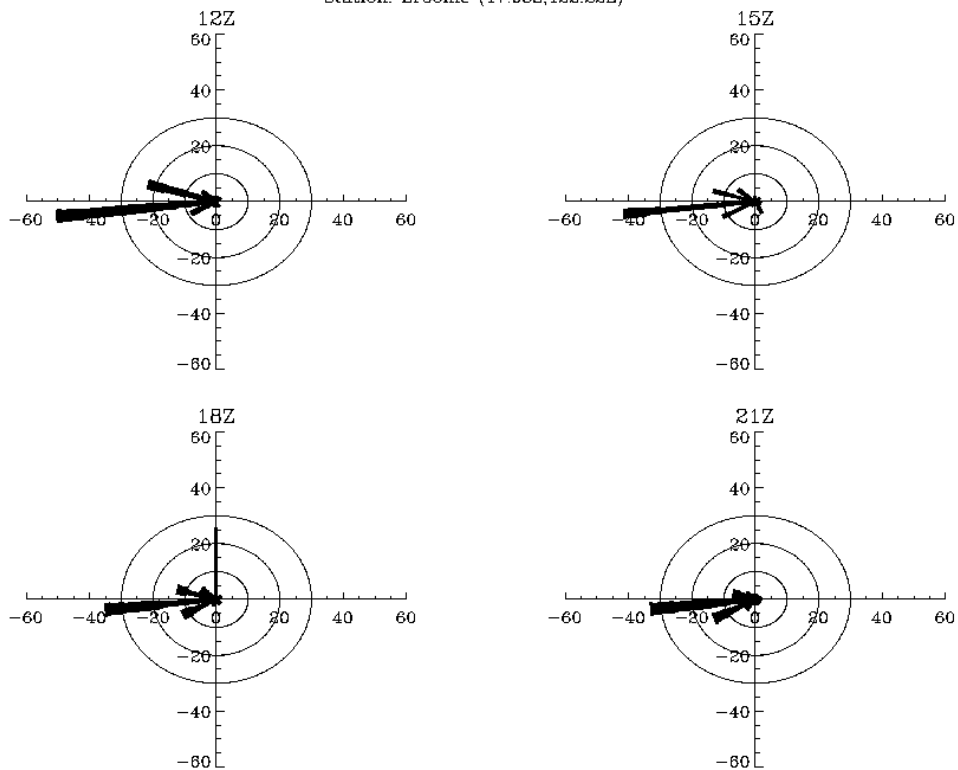
Station Bauerfield (91557) diurnal changes

Station: Broome (17.95S,122.22E)



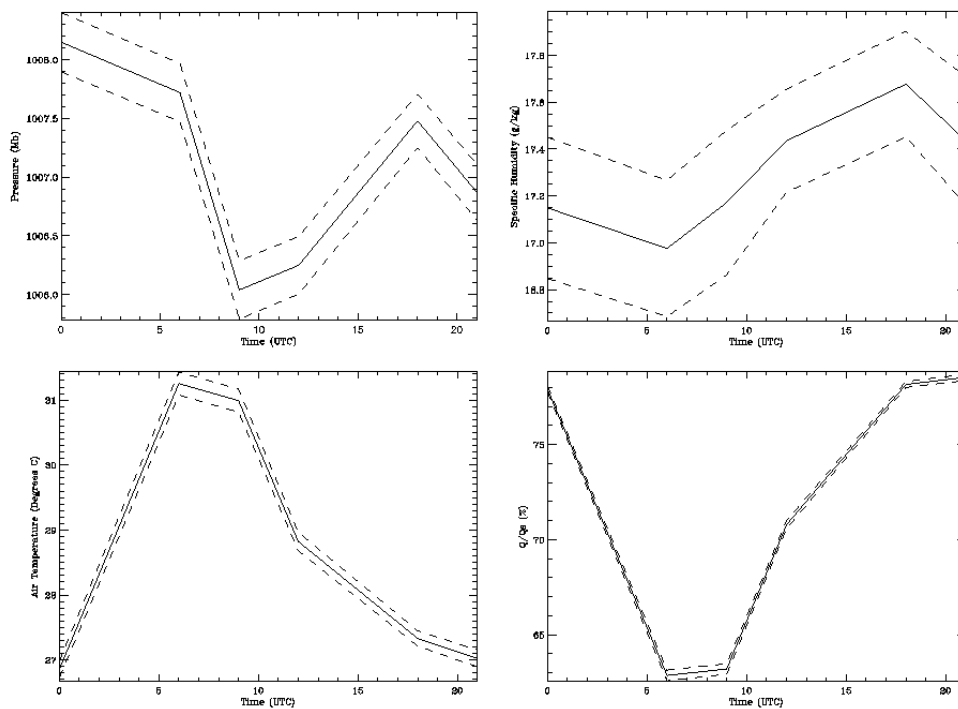
Station Broome (94203) 0,3,6,9 UTC Wind Roses

Station: Broome (17.95S,122.22E)



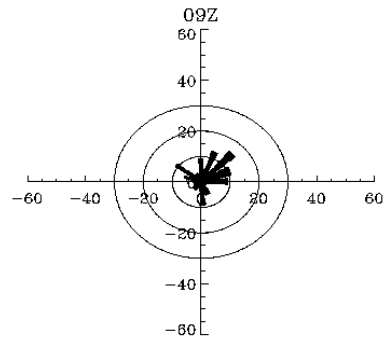
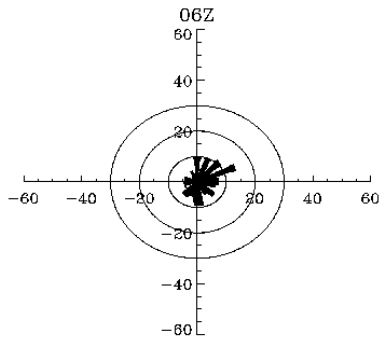
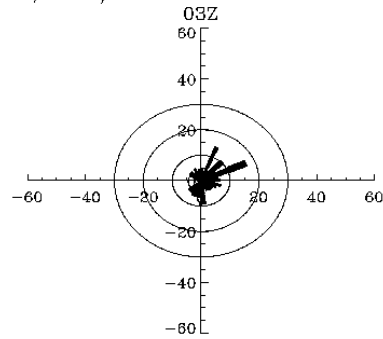
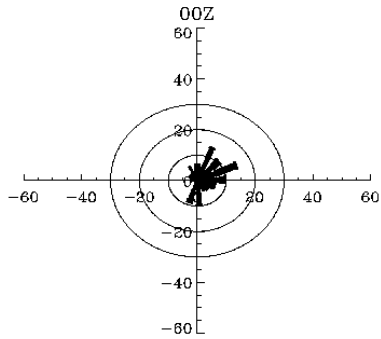
Station Broome (94203) 12,15,18,21 UTC Wind Roses

Station: Broome (17.95S 122.22E)



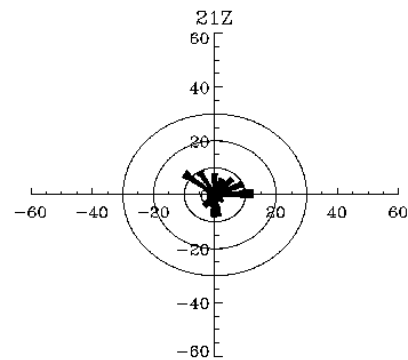
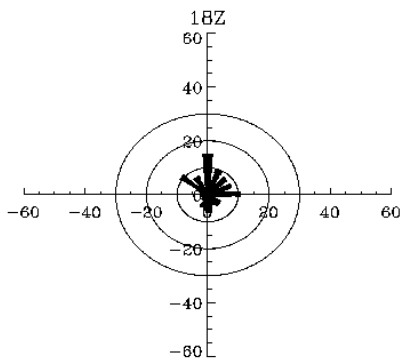
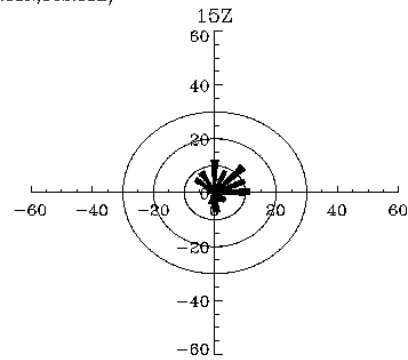
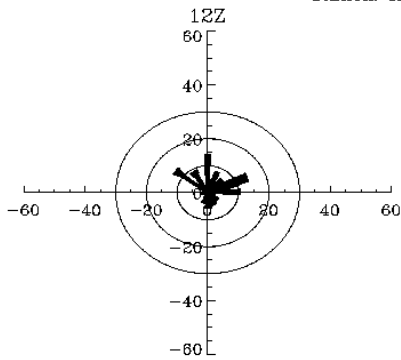
Station Broome (94203) diurnal changes

Station: Chichijima (27.08N,142.18E)



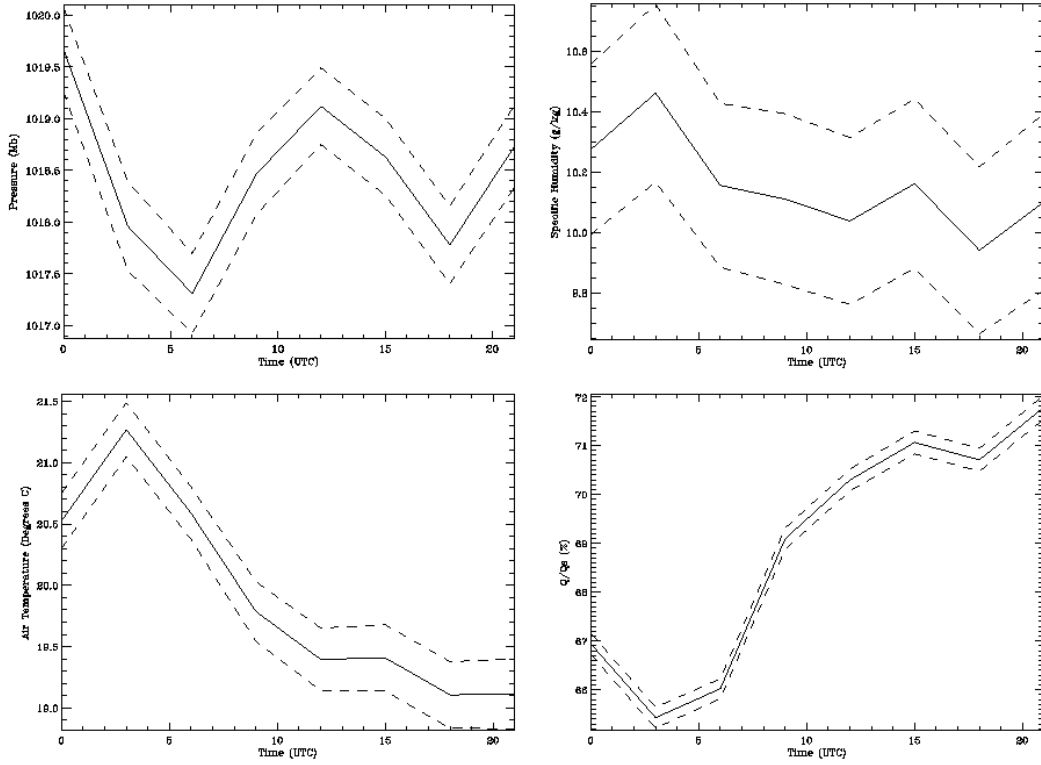
Station Chichijima (47971) 0,3,6,9 UTC Wind Roses

Station: Chichijima (27.08N,142.18E)



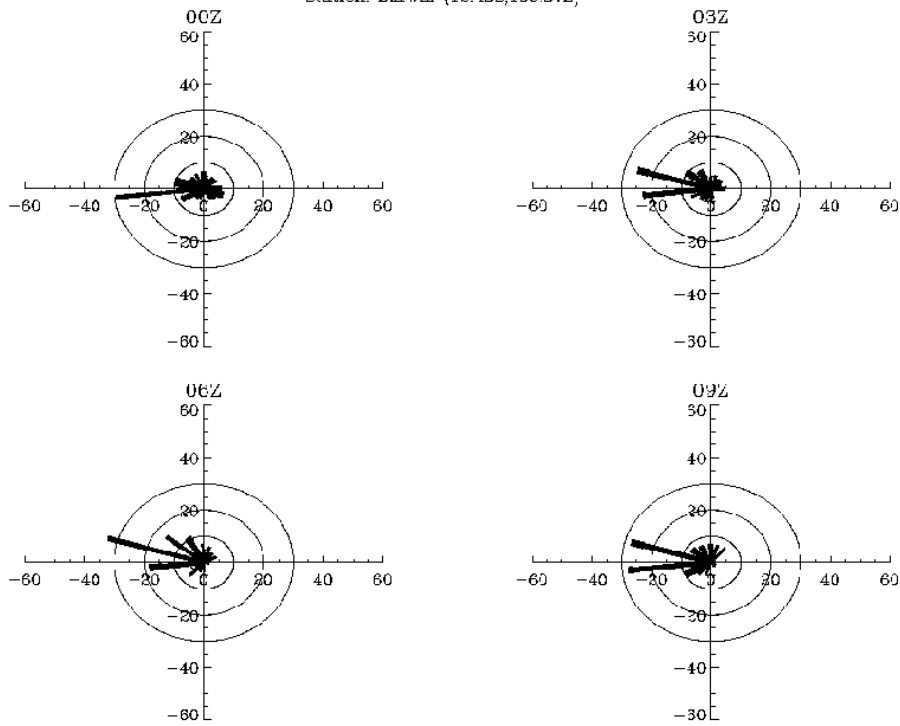
Station Chichijima (47971) 12,15,18,21 UTC Wind Roses

Station: Chichijima (27.08N 142.18E)



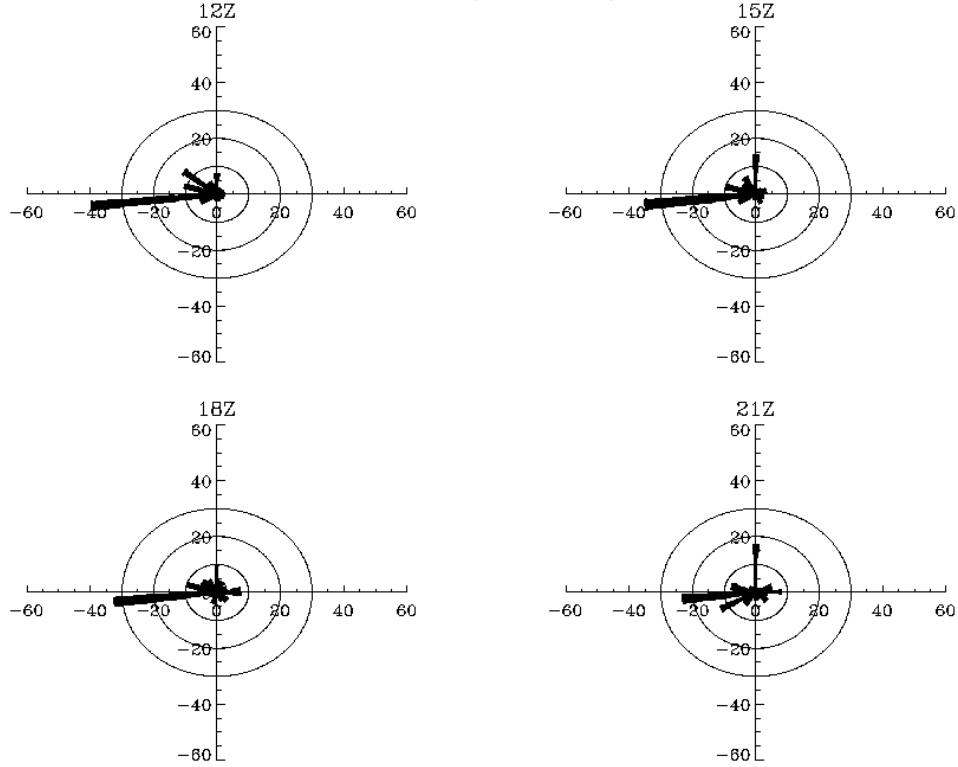
Station Chichijima (47971) diurnal changes

Station: Darwin (12.433,130.07E)



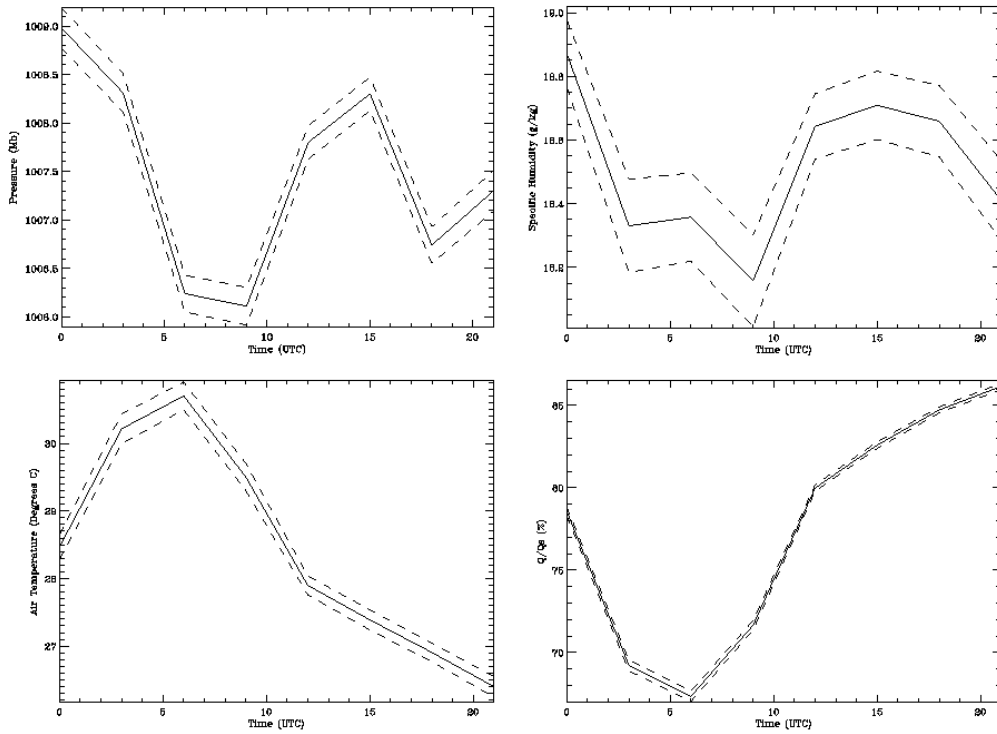
Station Darwin (94120) 0,3,6,9 UTC Wind Roses

Station: Darwin (12.43S,130.87E)



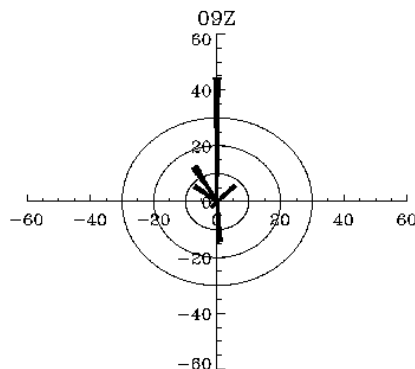
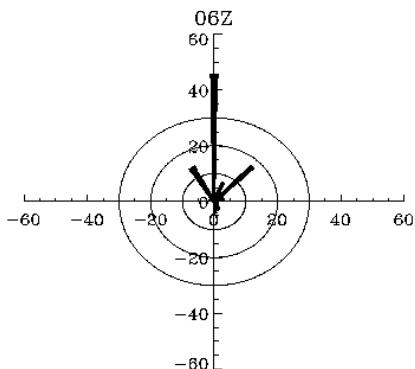
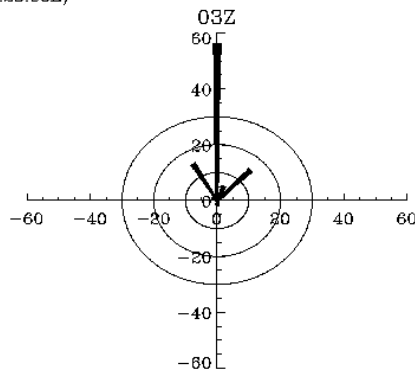
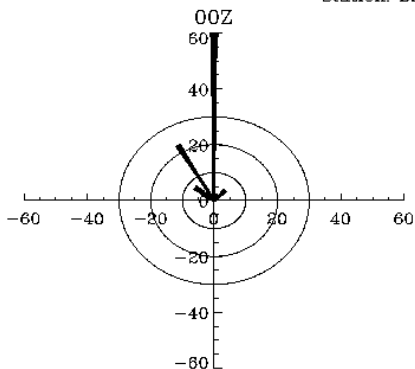
Station Darwin (94120) 12,15,18,21 UTC Wind Roses

Station: Darwin (12.43S 130.87E)



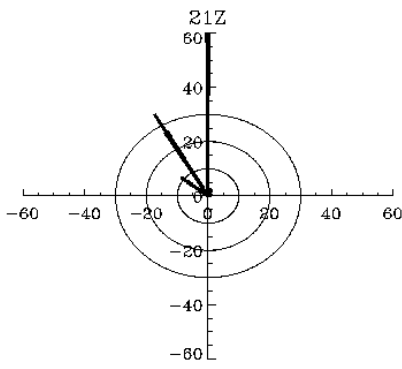
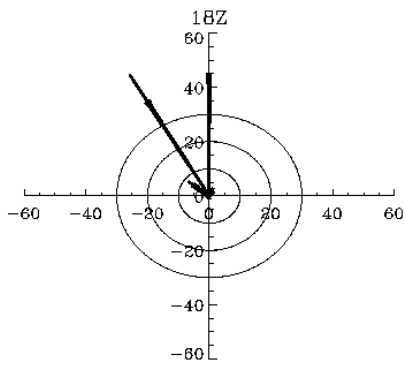
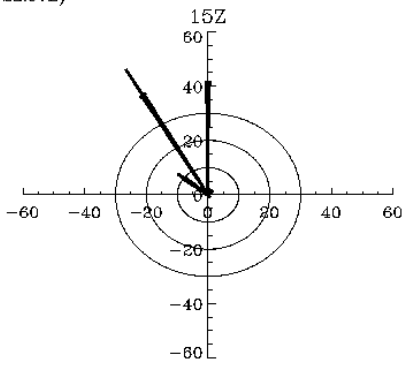
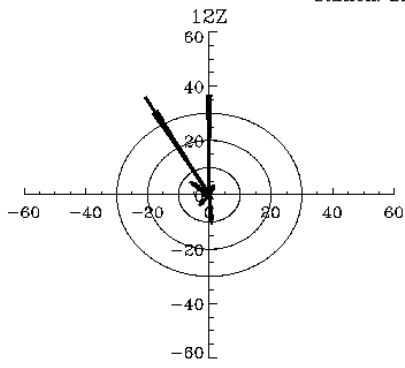
Station Darwin (94120) diurnal changes

Station: Davao (7.12N,125.65E)



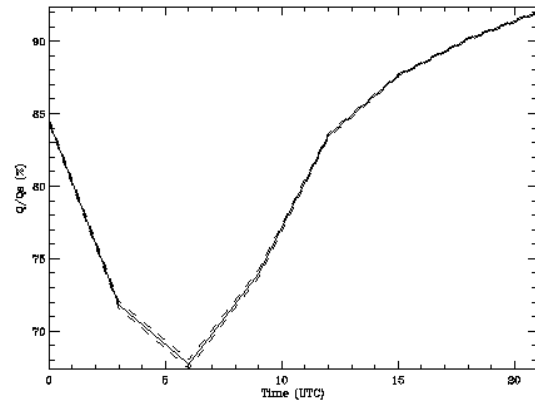
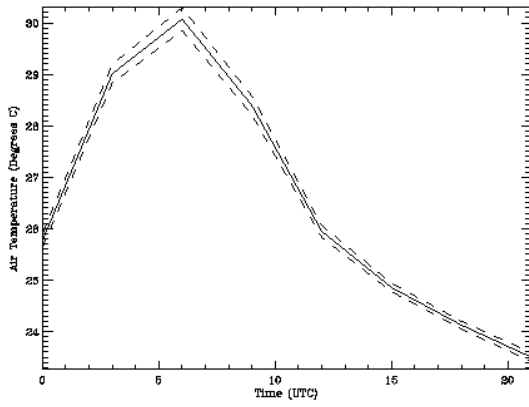
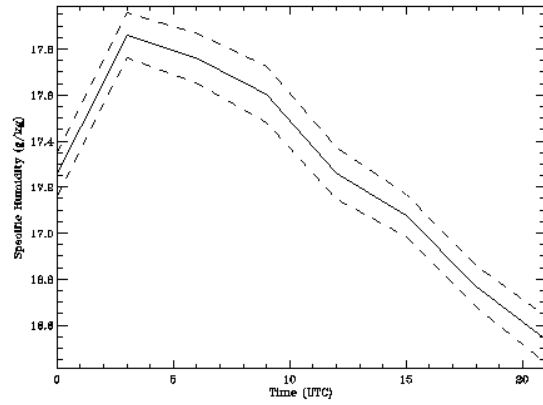
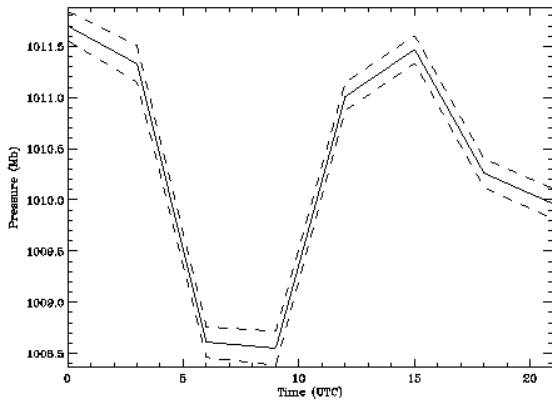
Station Davao (98753) 0,3,6,9 UTC Wind Roses

Station: Davao (10.30N,123.97E)



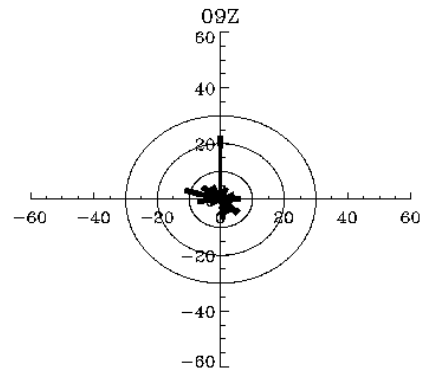
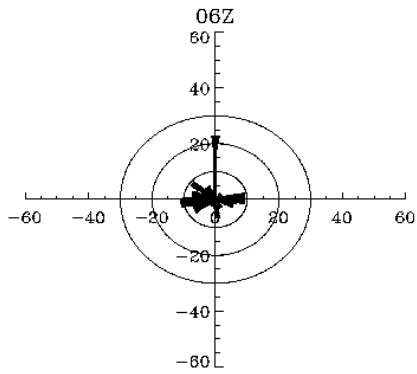
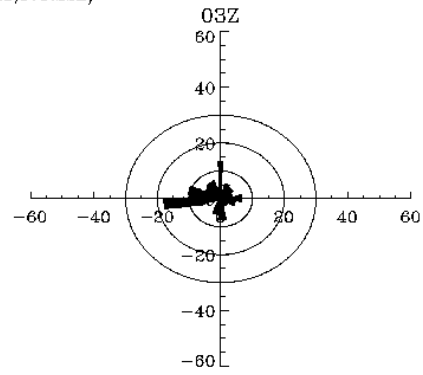
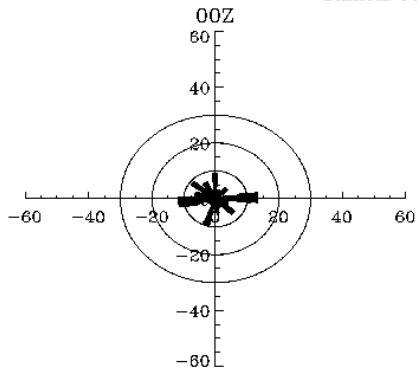
Station Davao (98753) 12,15,18,21 UTC Wind Roses

Station: Davao (7.12N 125.65E)



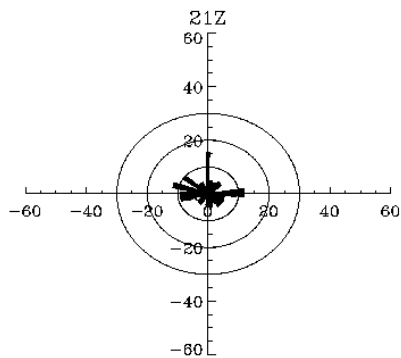
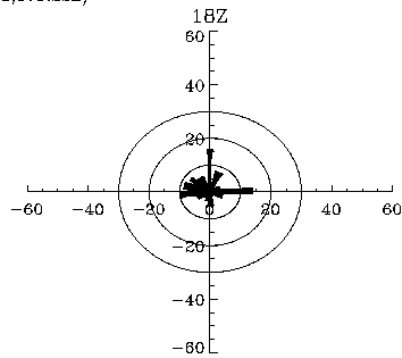
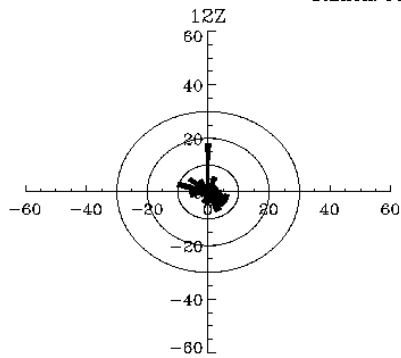
Station Davao (98753) diurnal changes

Station: Funafuti (8.52S,179.22E)



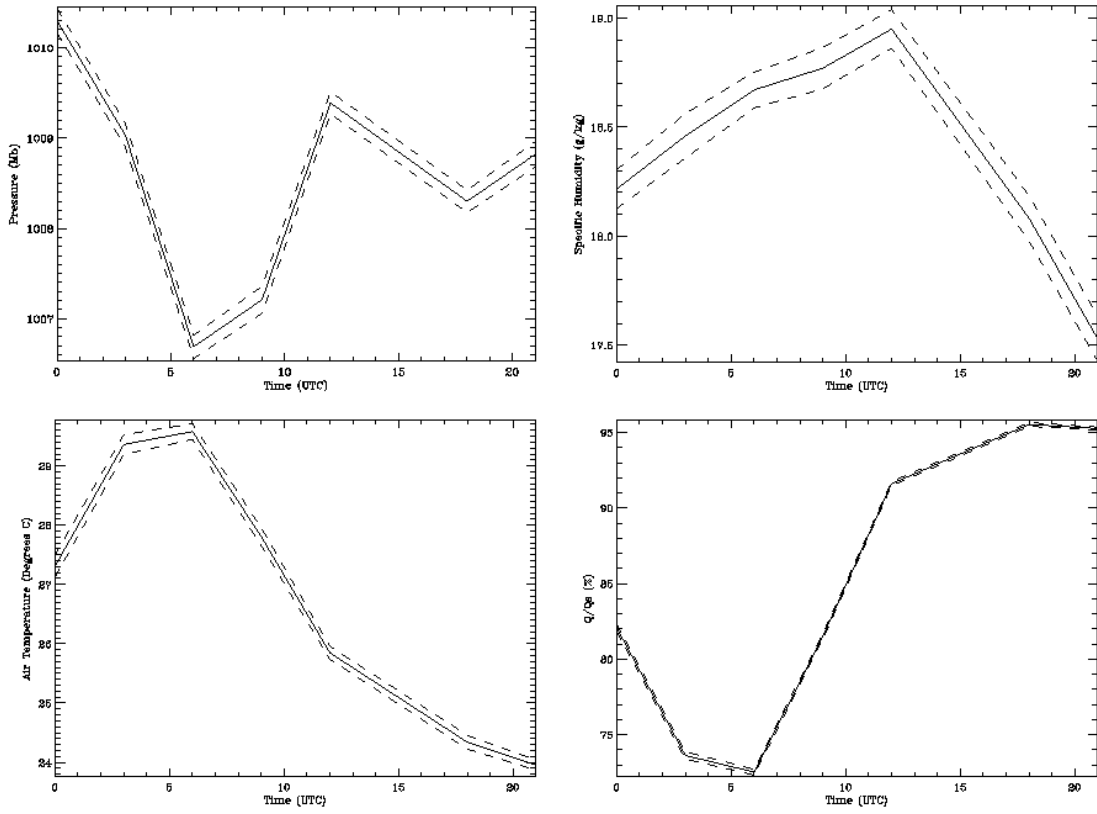
Station Funafuti (91643) 0,3,6,9 UTC Wind Roses

Station: Funafuti (8.52S,179.22E)



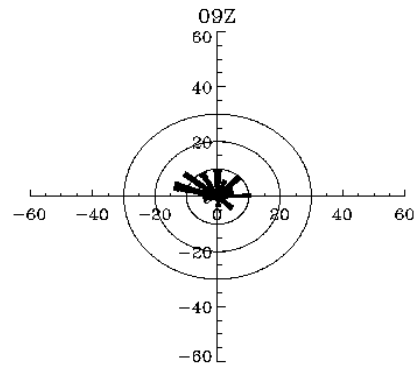
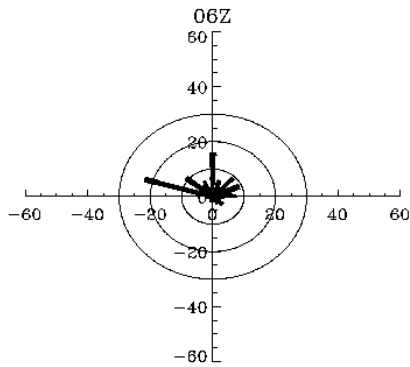
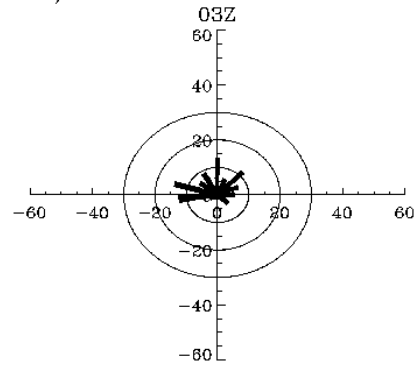
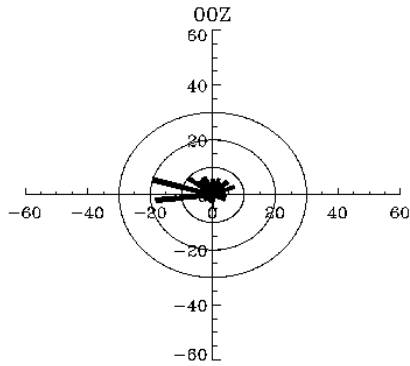
Station Funafuti (91643) 12,15,18,21 UTC Wind Roses

Station: Funafuti (8.52S 179.22E)



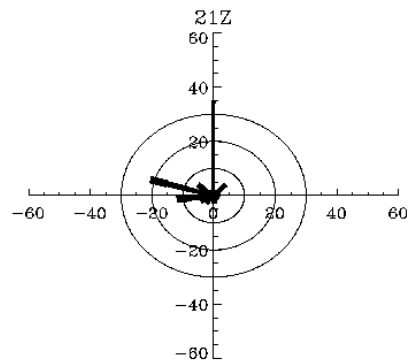
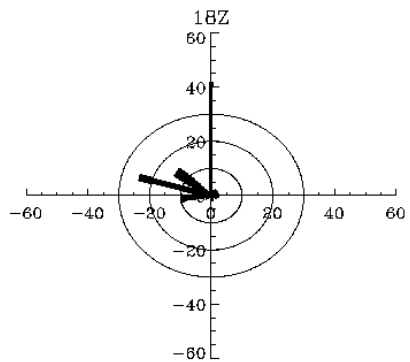
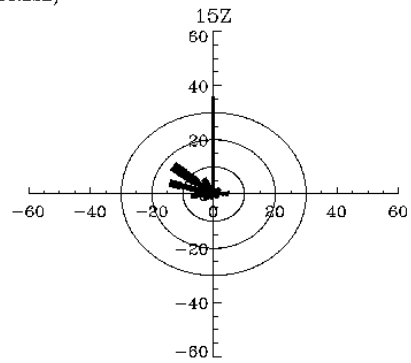
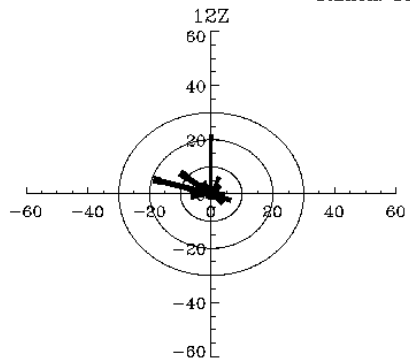
Station Funafuti (91643) diurnal changes

Station: Gove (12.28S,136.82E)



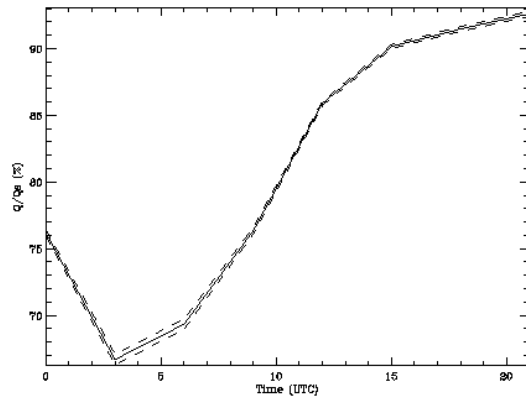
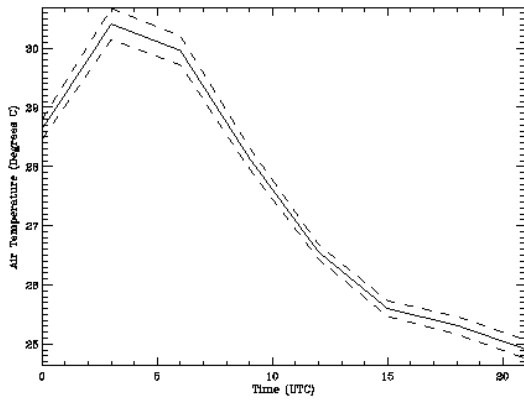
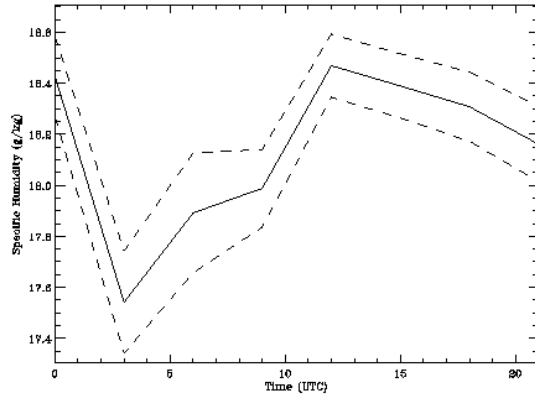
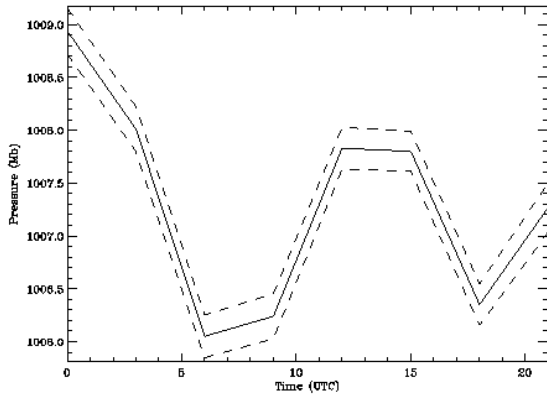
Station Gove (94150) 0,3,6,9 UTC Wind Roses

Station: Gove (12.28S,136.82E)



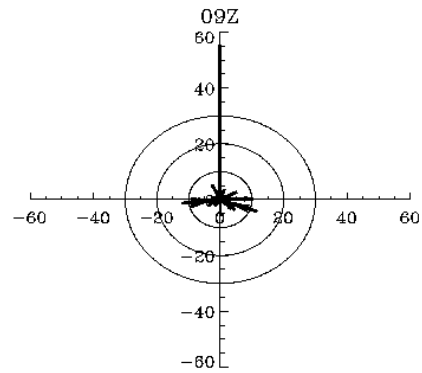
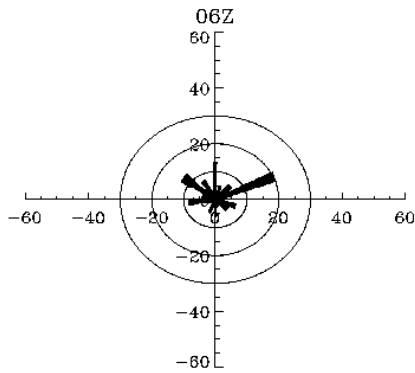
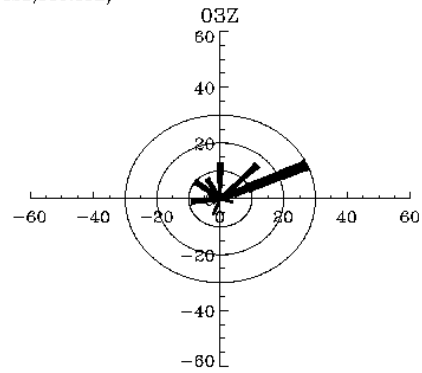
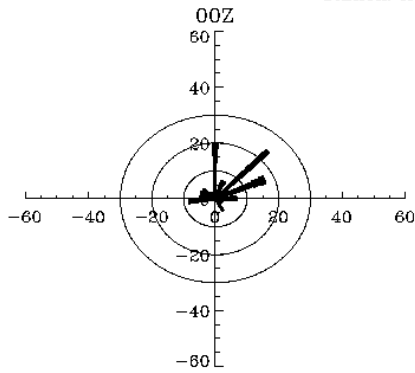
Station Gove (94150) 12,15,18,21 UTC Wind Roses

Station: Gove (12.26S 136.82E)



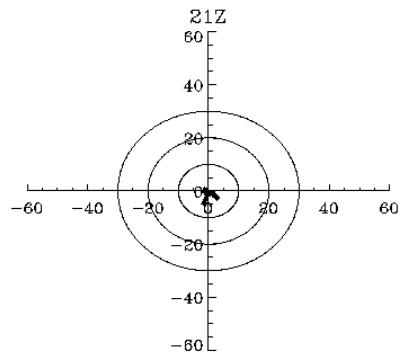
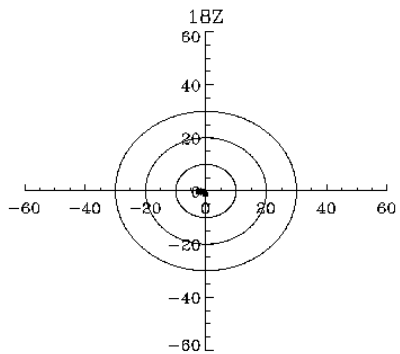
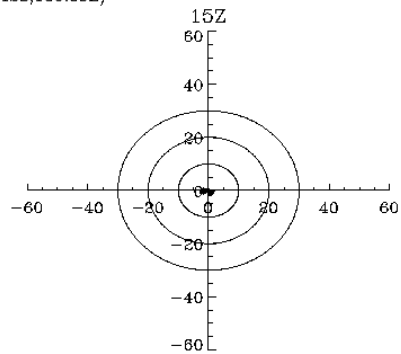
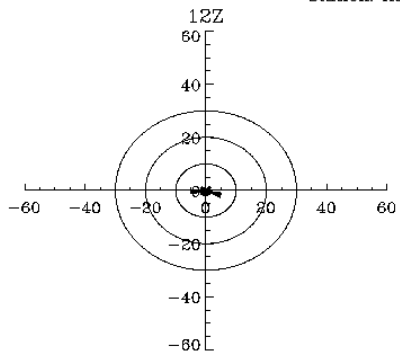
Station Gove (94150) diurnal changes

Station: Henderson (9.42S,160.05E)



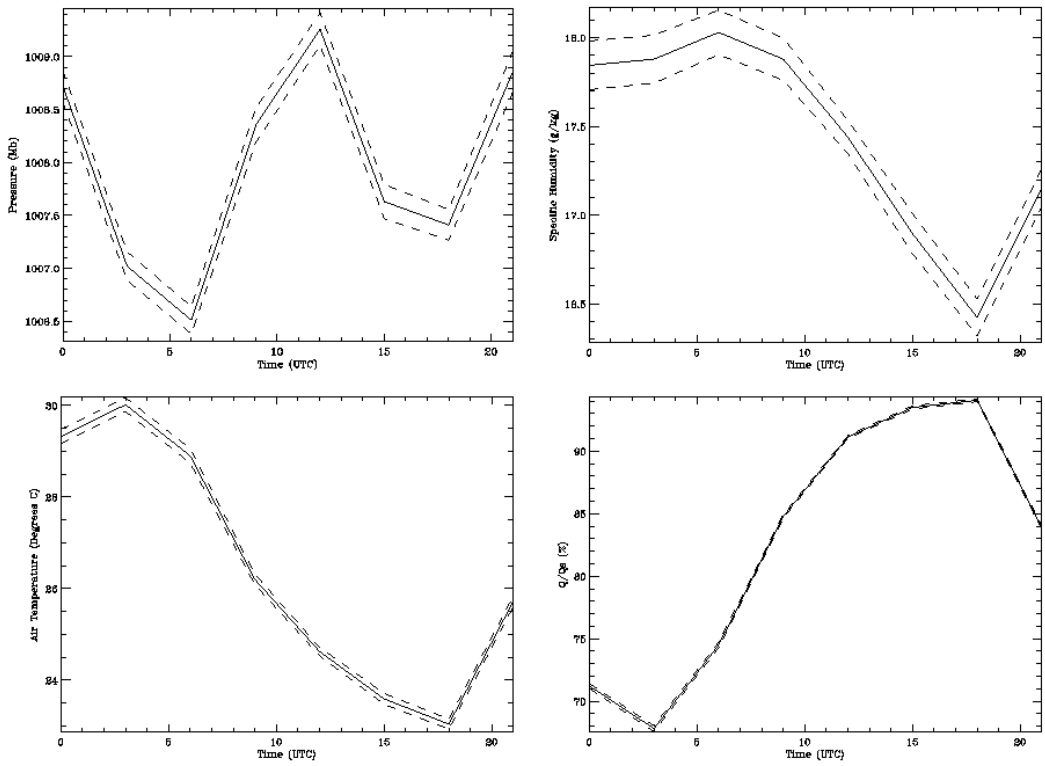
Station Henderson (91520) 0,3,6,9 UTC Wind Roses

Station: Henderson (9.42S,160.05E)



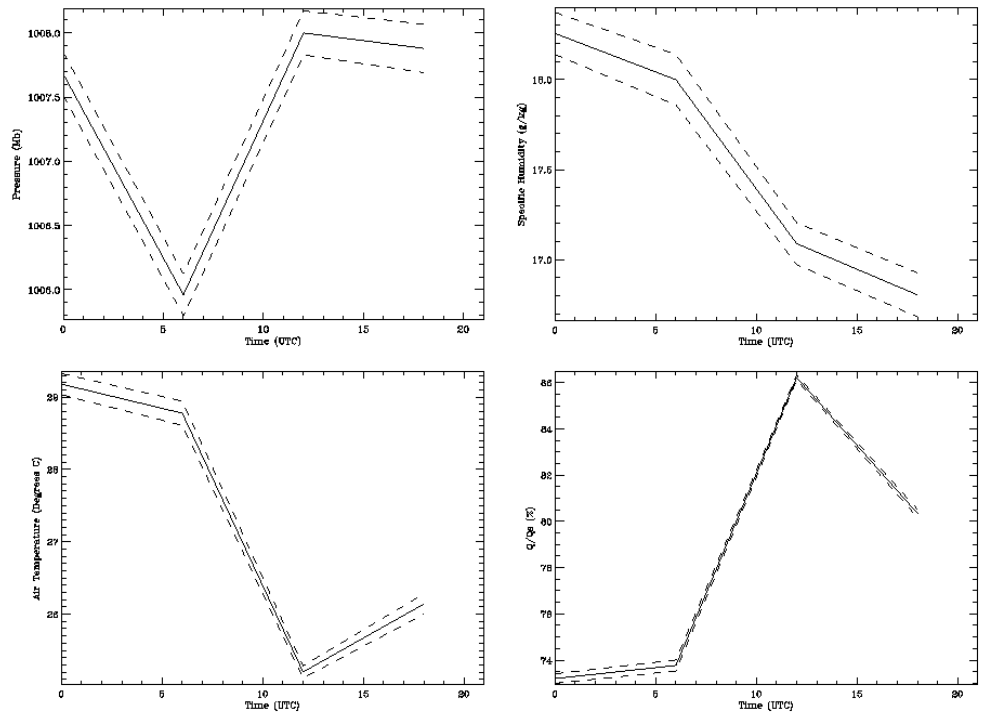
Station Henderson (91520) 12,15,18,21 UTC Wind Roses

Station: Henderson (9.42S 160.05E)



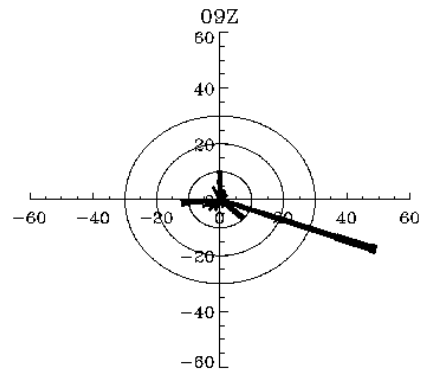
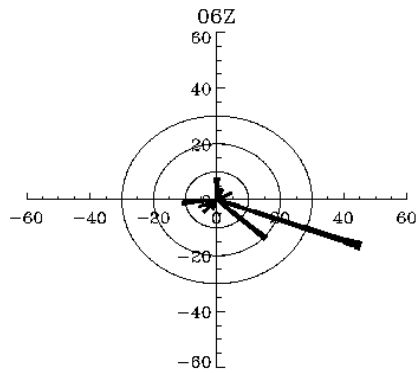
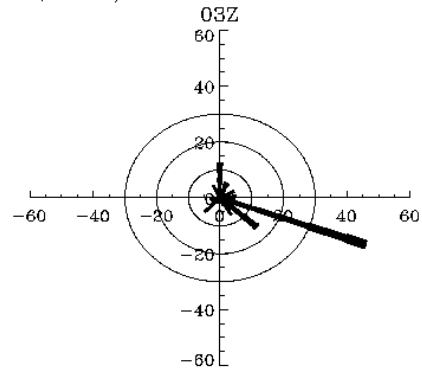
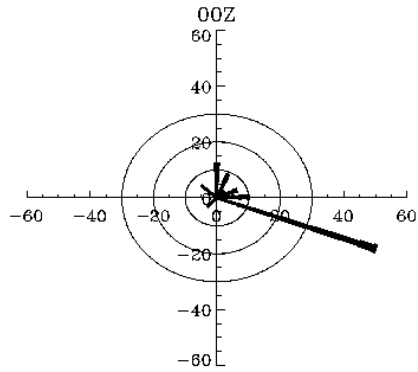
Station Henderson (91520) diurnal changes

Station: Honiara (9.42S 159.97E)



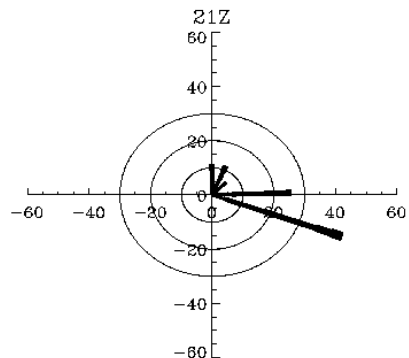
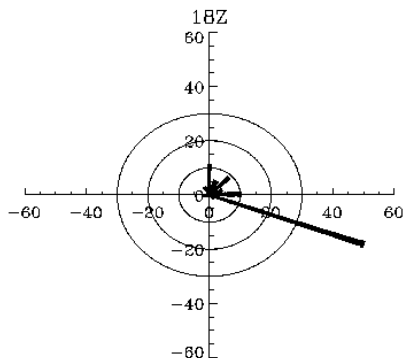
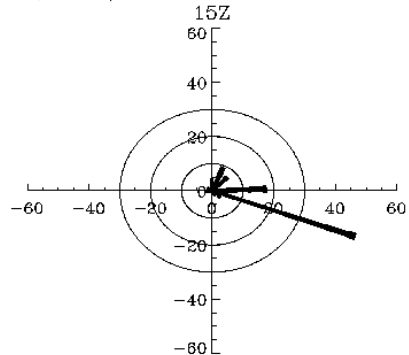
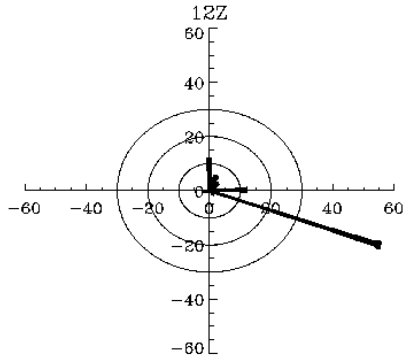
Station Honiara (91517) diurnal changes

Station: Kings_Park (22.32N,114.17E)



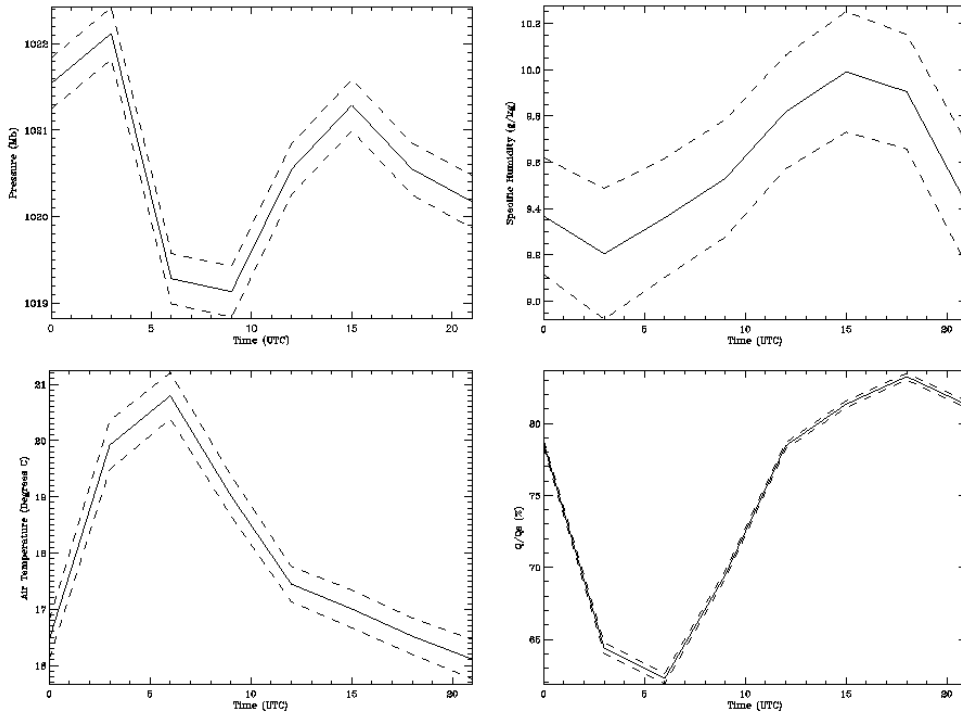
Station King's Park (45004) 0,3,6,9 UTC Wind Roses

Station: Kings_Park (22.32N,114.17E)



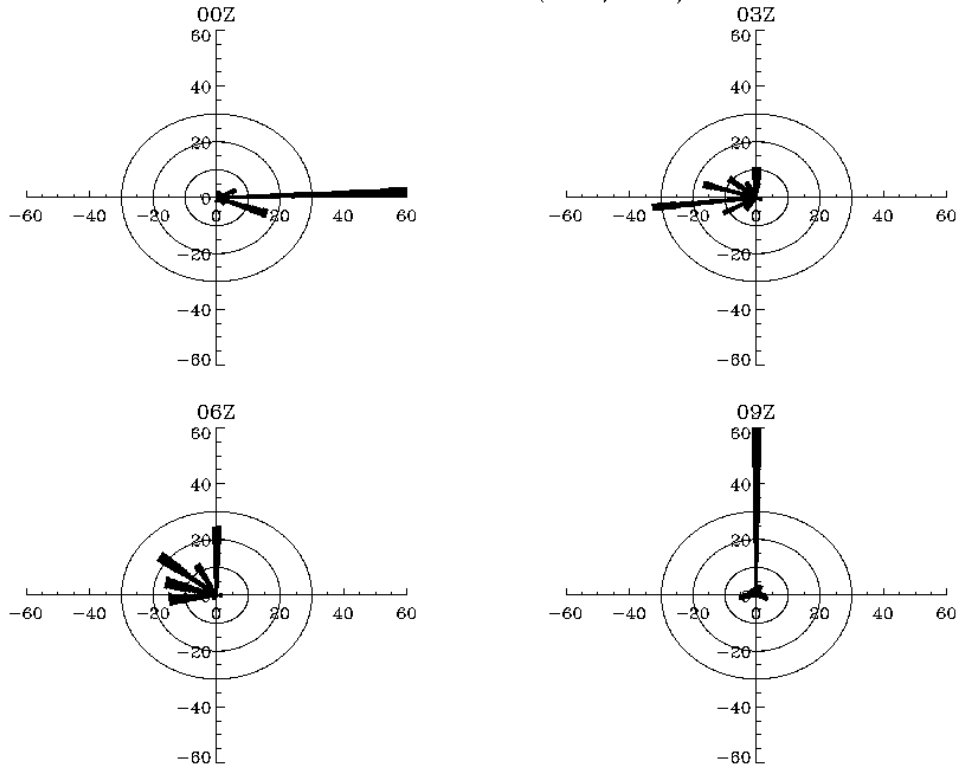
Station King's Park (45004) 12,15,18,21 UTC Wind Roses

Station: Kings_Park (22.32N 114.17E)



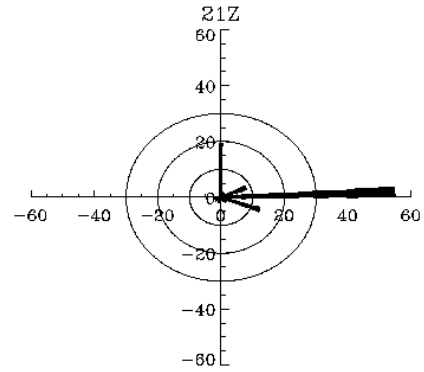
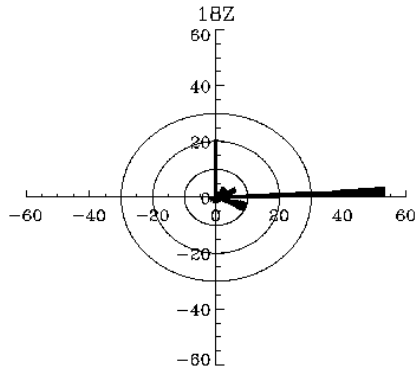
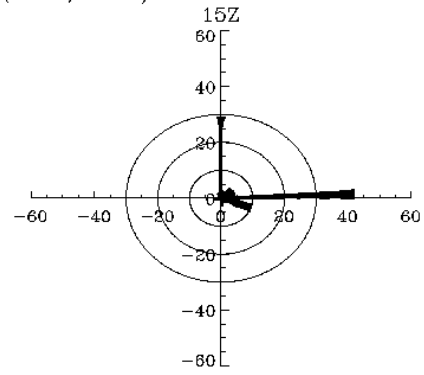
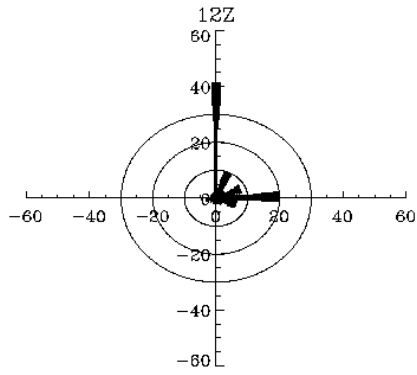
Station King's Park (45004) diurnal changes

Station: Kota_Kinabalu (1.46N,110.33E)



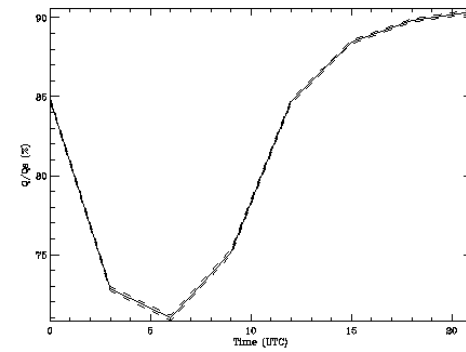
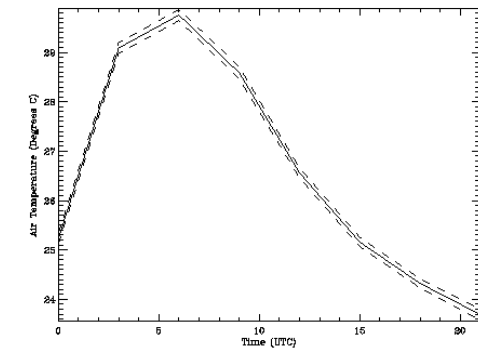
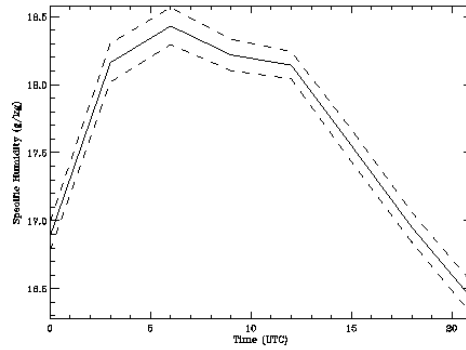
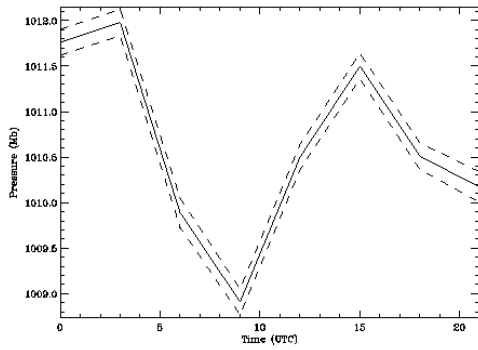
Station Kota Kinabalu (96471) 0,3,6,9 UTC Wind Roses

Station: Kota_Kinabalu (1.48N,110.33E)



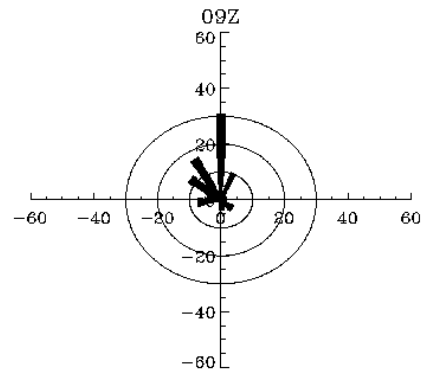
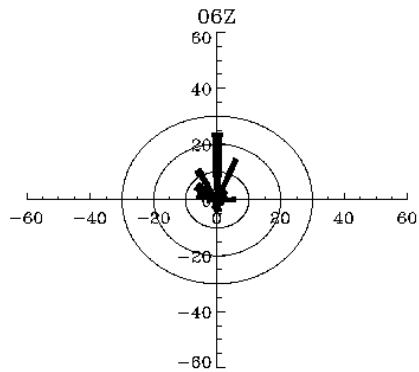
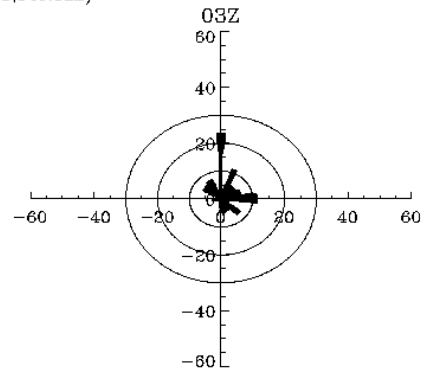
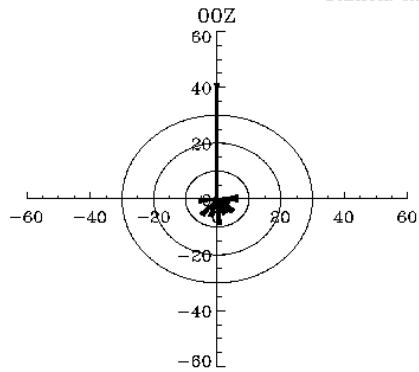
Station Kota Kinabalu (96471) 12,15,18,21 UTC Wind Roses

Station: Kota-Kinabalu (5.95N 116.05E)



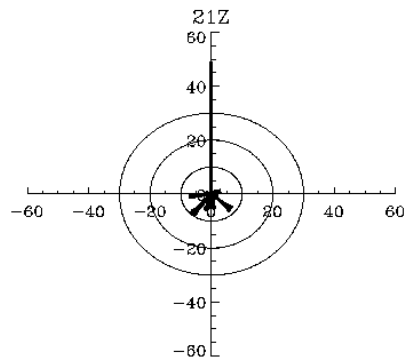
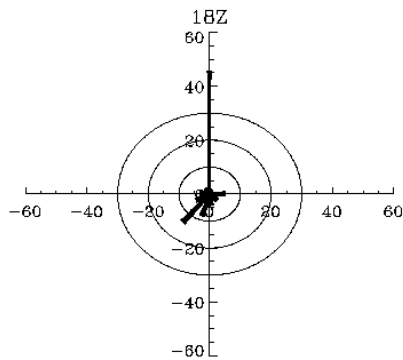
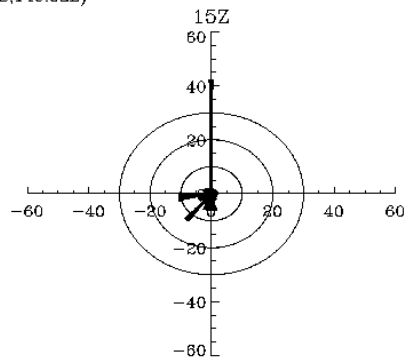
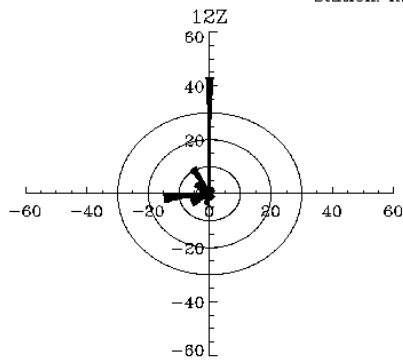
Station Kota Kinabalu (96471) diurnal changes

Station: Kuching (16.30S,149.98E)



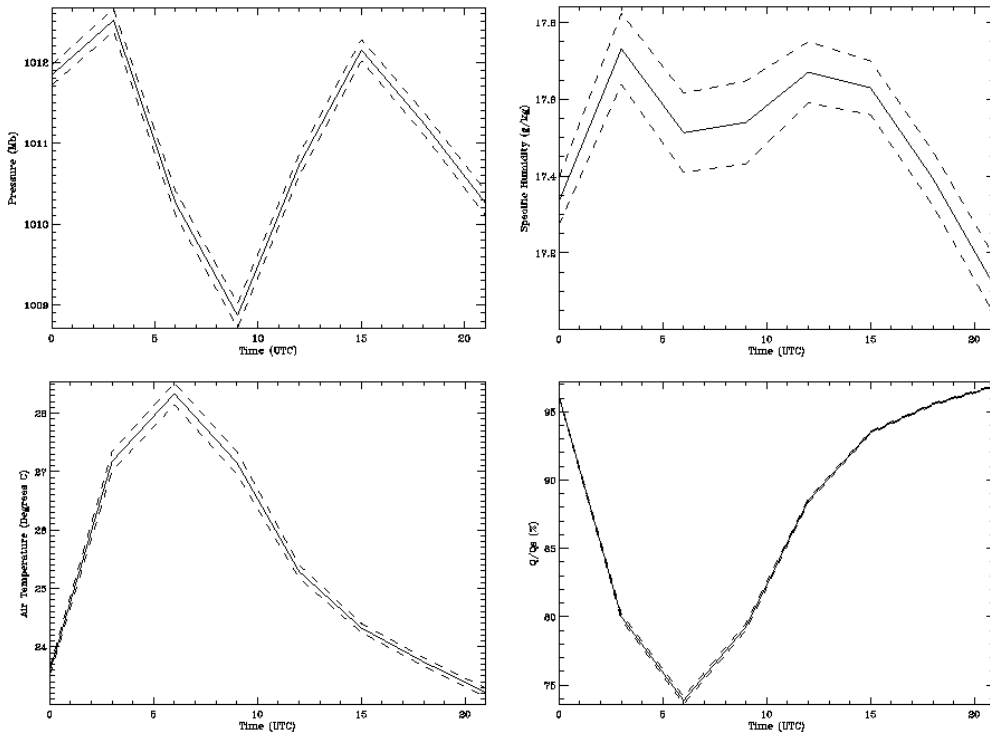
Station Kuching (96413) 0,3,6,9 UTC Wind Roses

Station: Kuching (16.30S,149.98E)



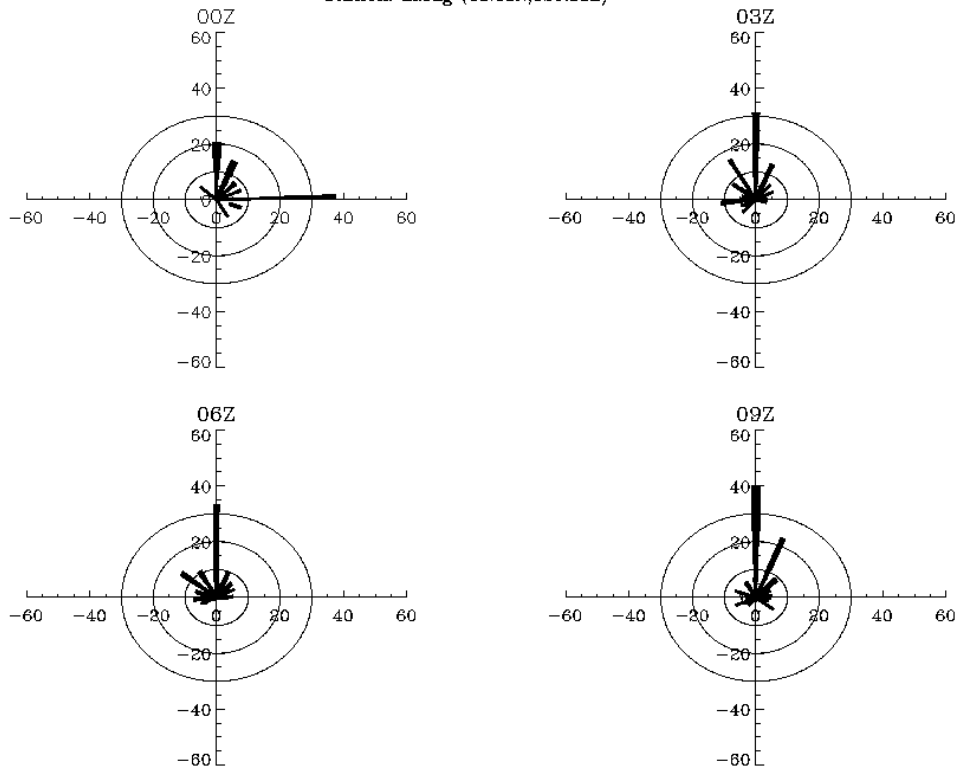
Station Kuching (96413) 12,15,18,21 UTC Wind Roses

Station: Kuching-In-Sarawak (1.48N 110.33E)



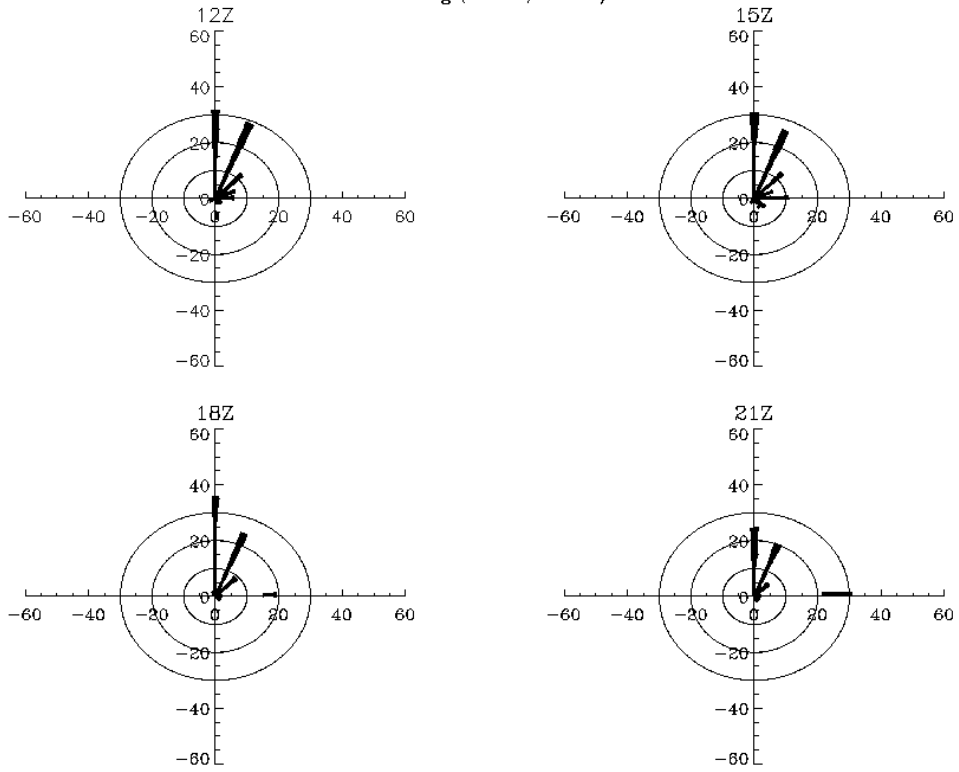
Station Kuching (96413) diurnal changes

Station: Laoag (18.18N,120.53E)



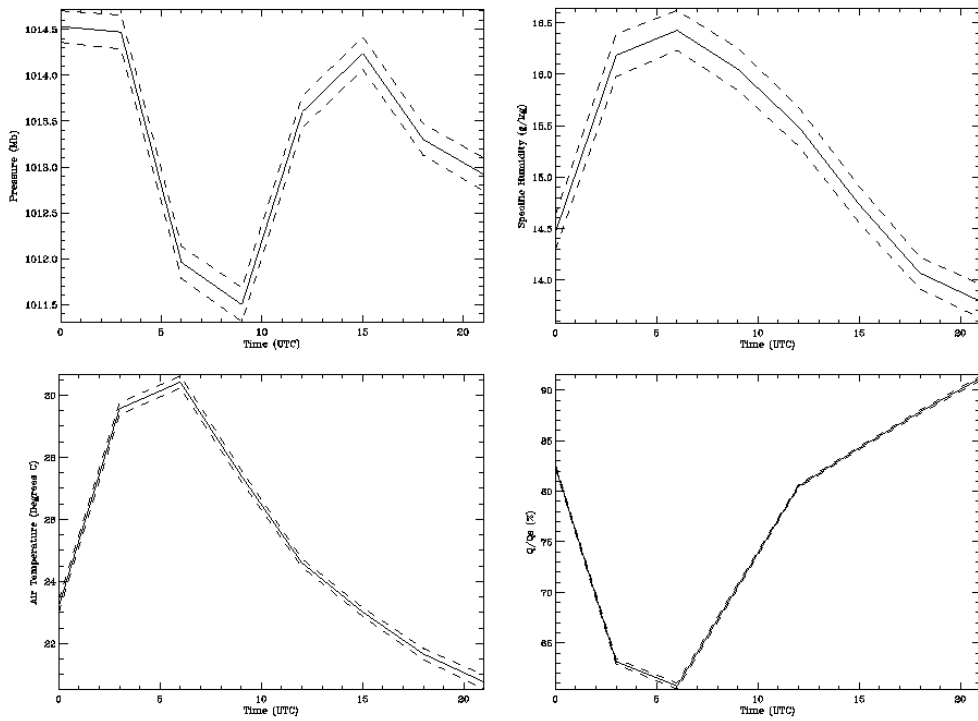
Station Laoag (98223) 0,3,6,9 UTC Wind Roses

Station: Laoag (18.18N,120.53E)



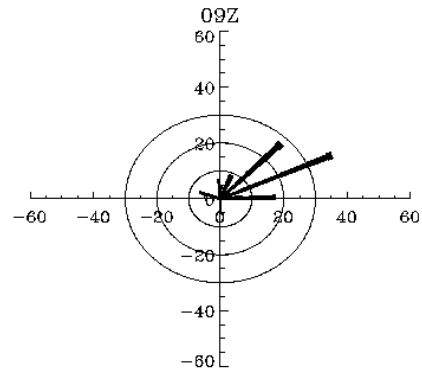
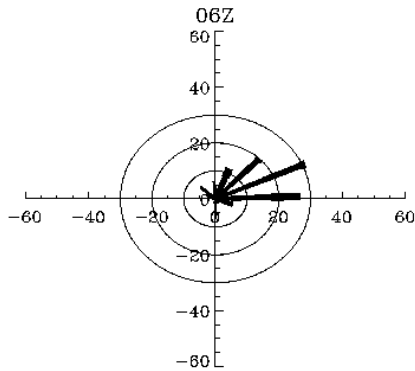
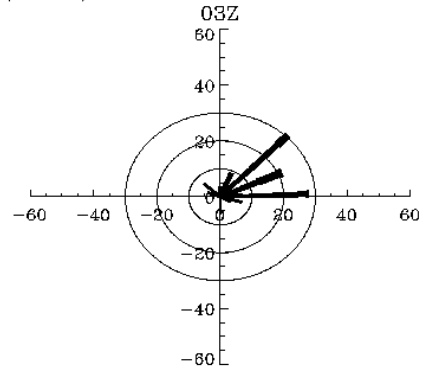
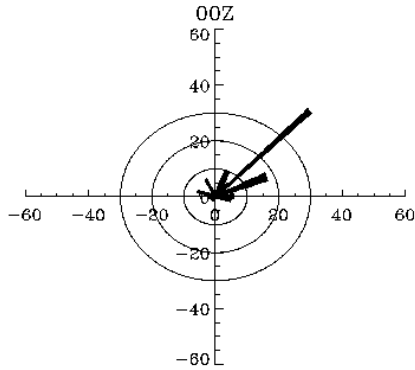
Station Laoag (98223) 12,15,18,21 UTC Wind Roses

Station: Laoag (18.18N 120.53E)



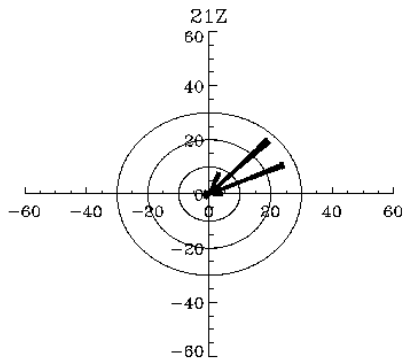
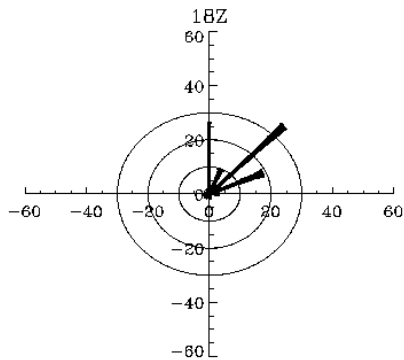
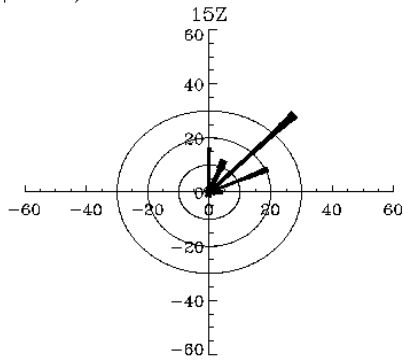
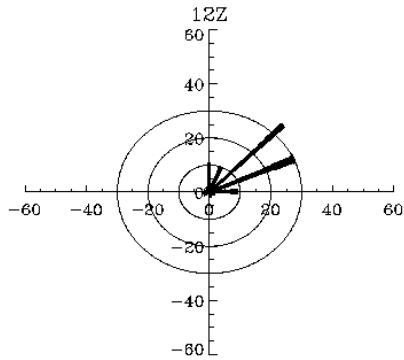
Station Laoag (98223) diurnal changes

Station: Legazpi (13.13N,123.73E)



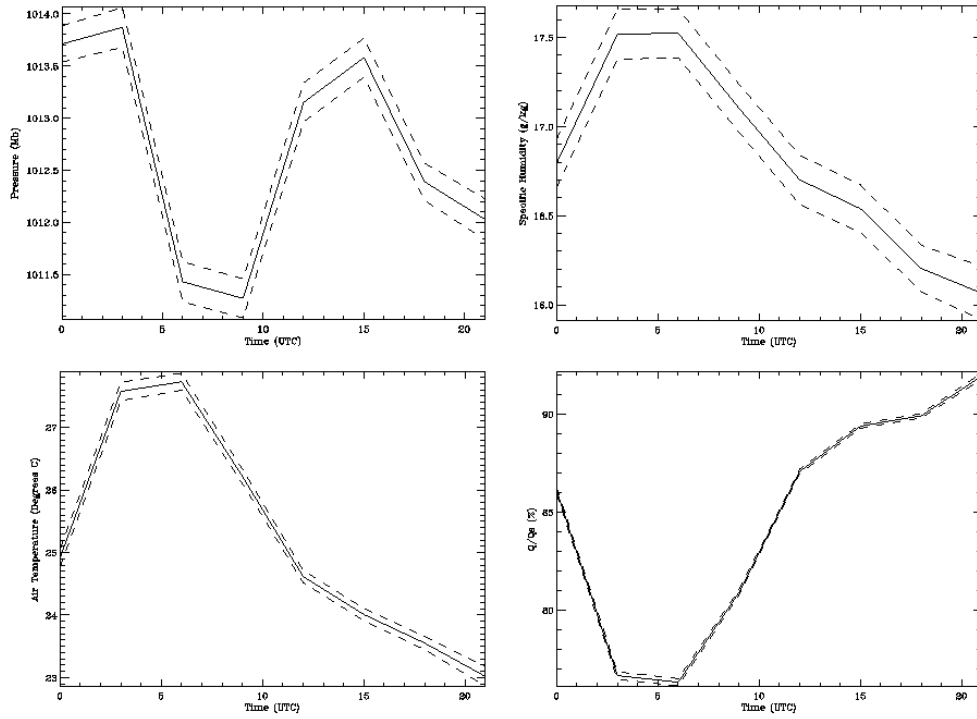
Station Legazpi (93444) 0,3,6,9 UTC Wind Roses

Station: Legazpi (13.13N,123.73E)



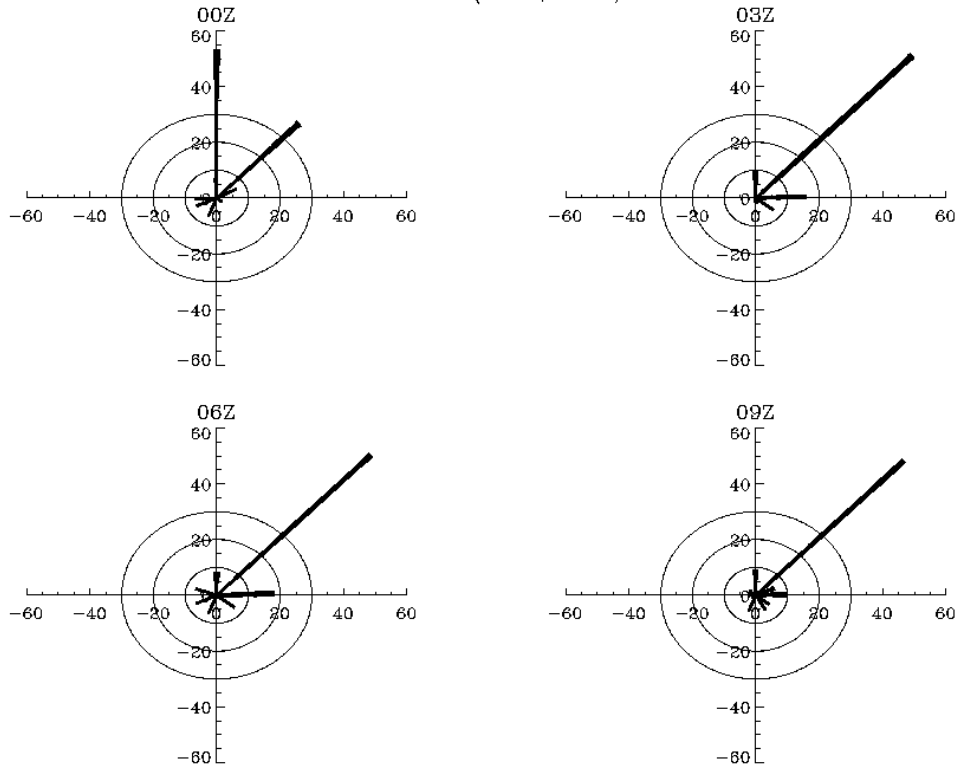
Station Legazpi (93444) 12,15,18,21 UTC Wind Roses

Station: Legazpi (13.13N 123.73E)



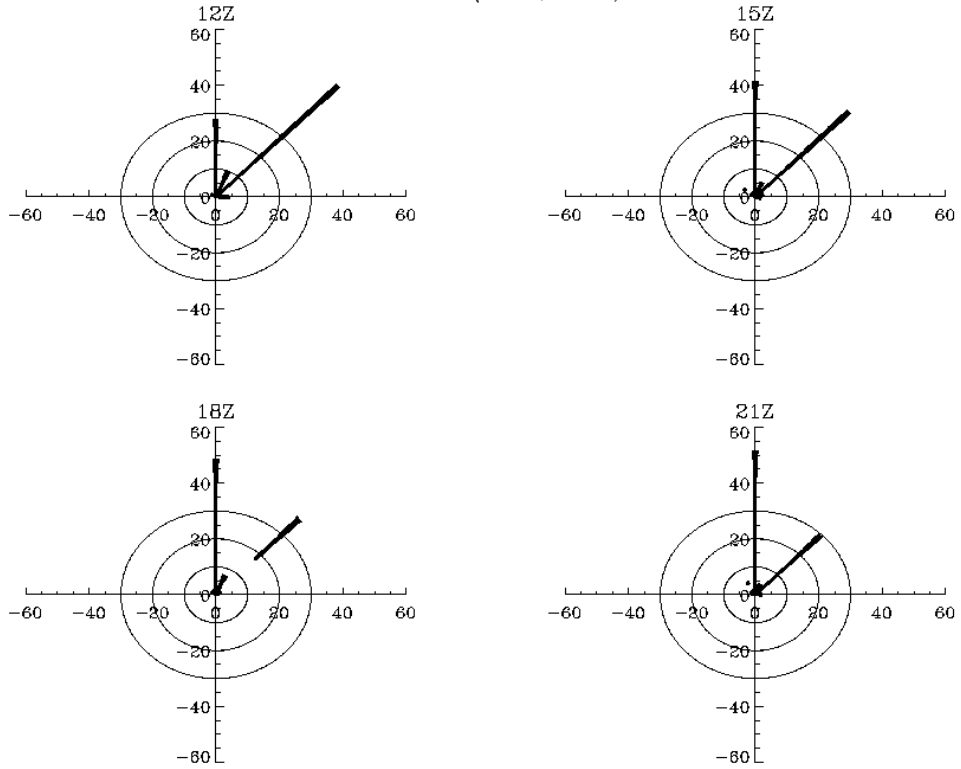
Station Legazpi (93444) diurnal changes

Station: Mactan (10.30N,123.97E)



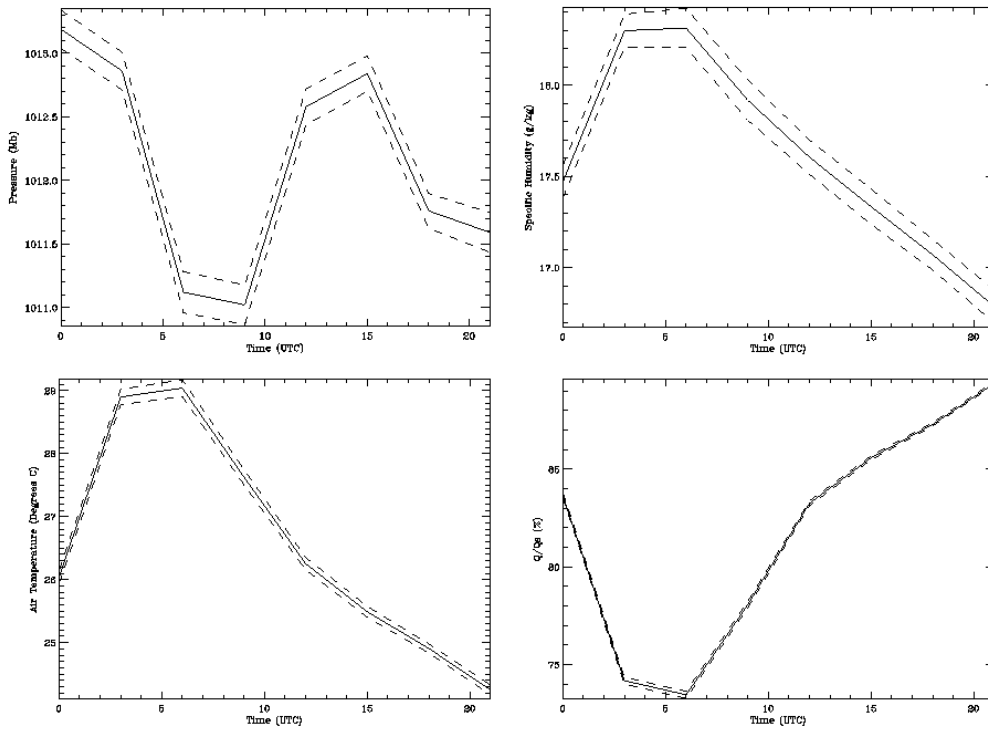
Station Mactan (98646) 0,3,6,9 UTC Wind Roses

Station: Mactan (10.30N,123.97E)



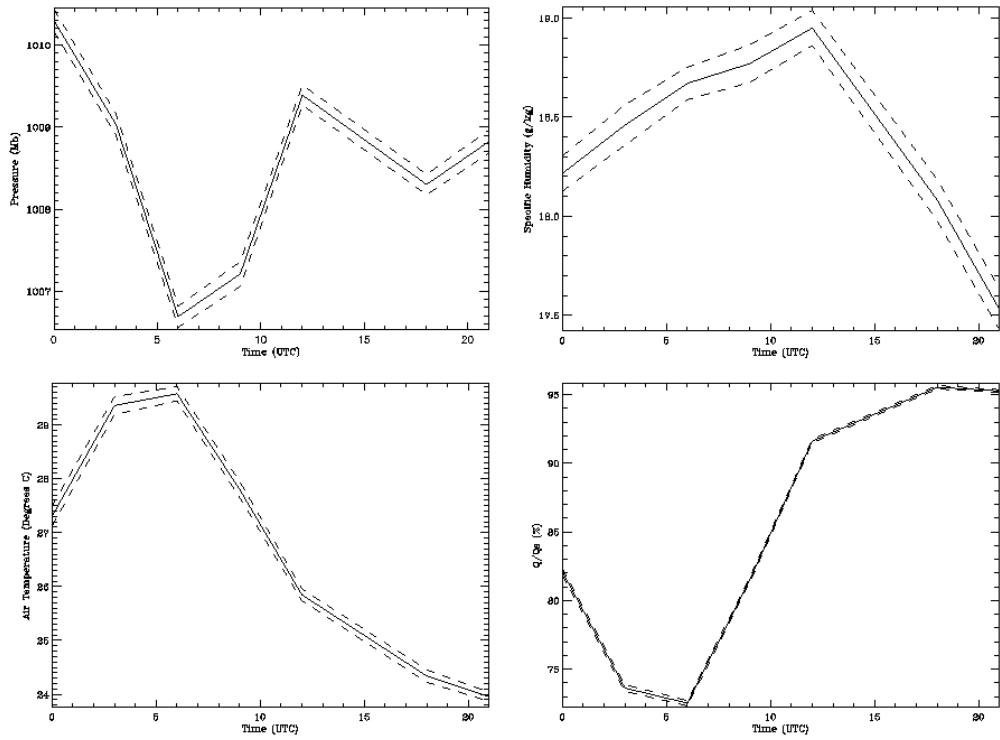
Station Mactan (98646) 12,15,18,21 UTC Wind Roses

Station: Mactan (10.30N 123.97E)



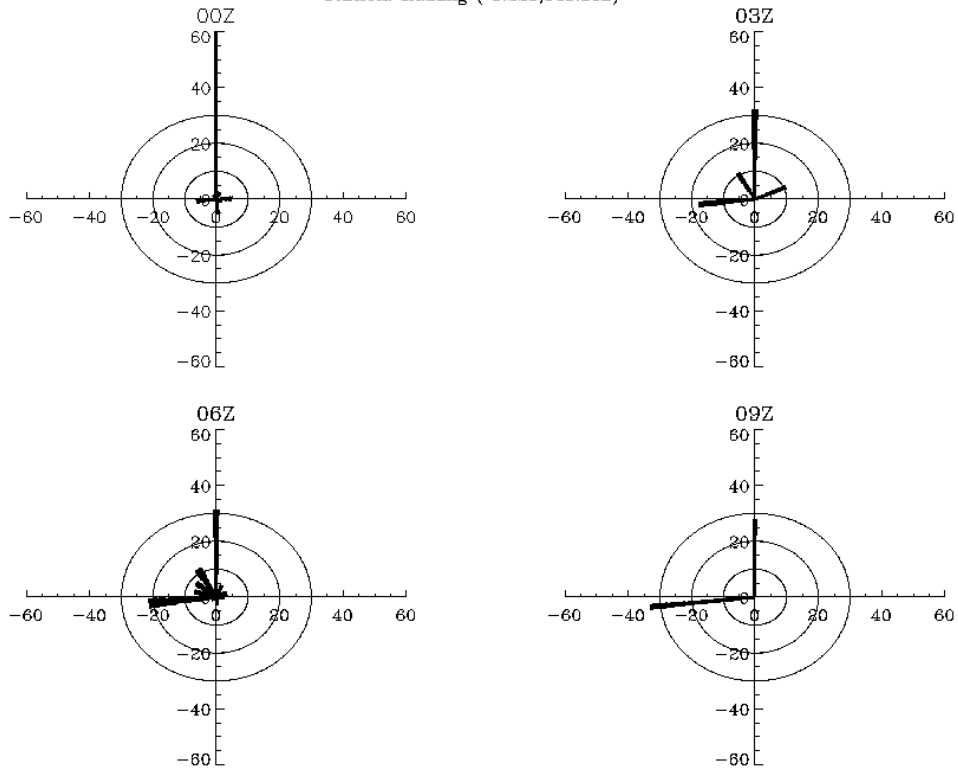
Station Mactan (98646) diurnal changes

Station: Madang (5.22S 145.80E)



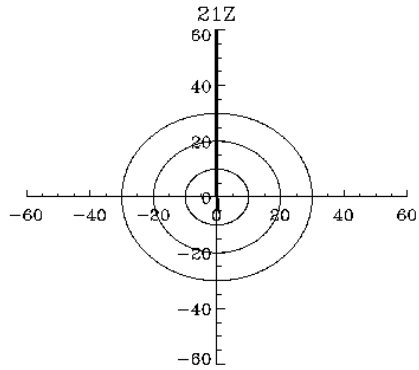
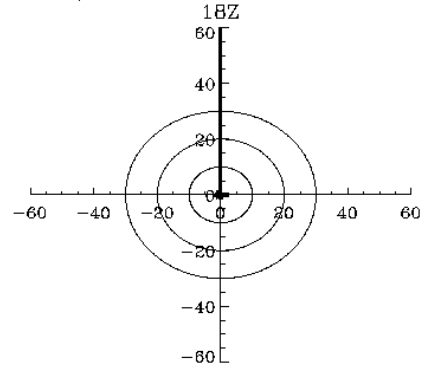
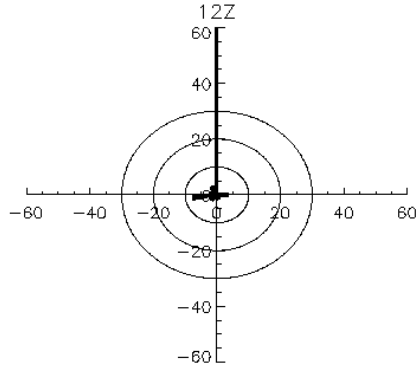
Station Madang (94014) diurnal changes

Station: Madang (5.22S,145.80E)



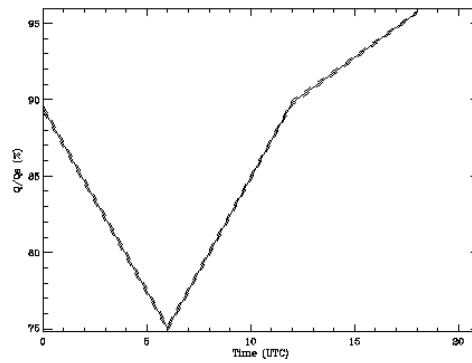
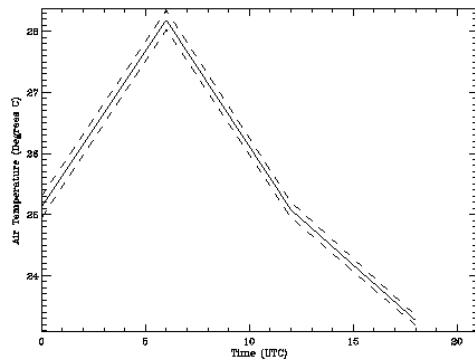
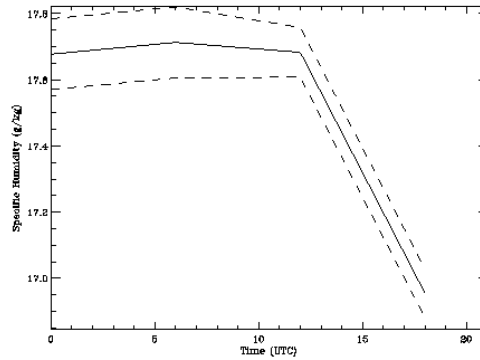
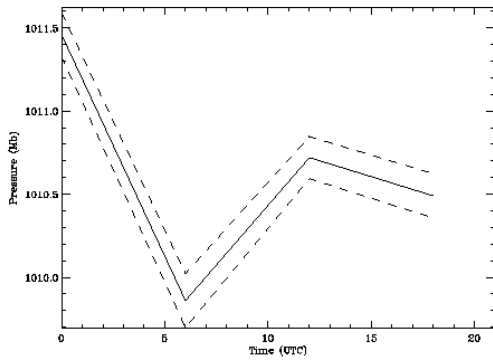
Station Madang (97014) 0,3,6,9 UTC Wind Roses

Station: Madang (5.22S,145.80E)



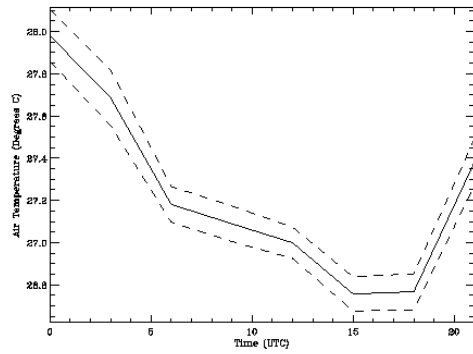
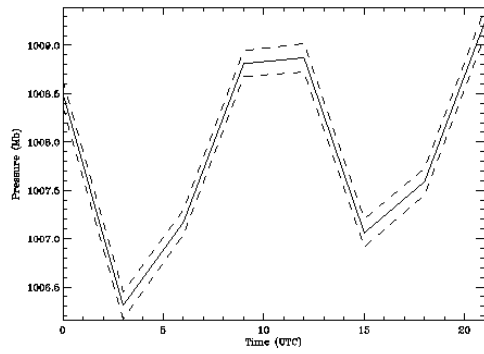
Station Madang (97014) 12,15,18,21 UTC Wind Roses

Station: Menado (1.53N 124.92E)



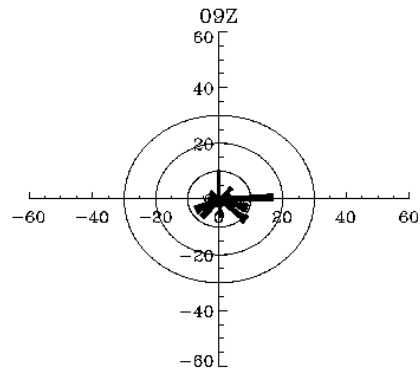
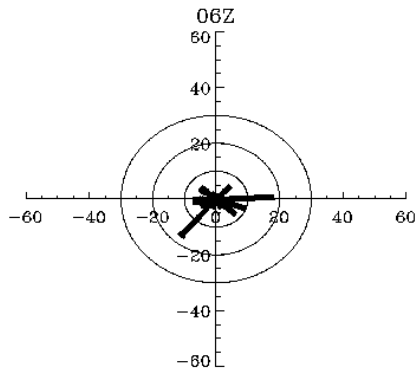
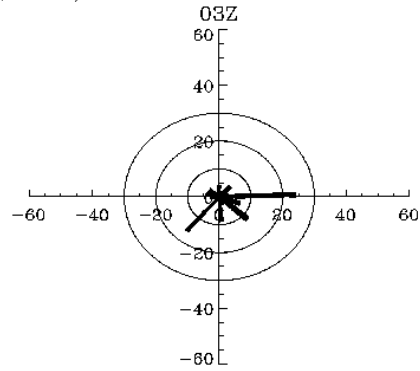
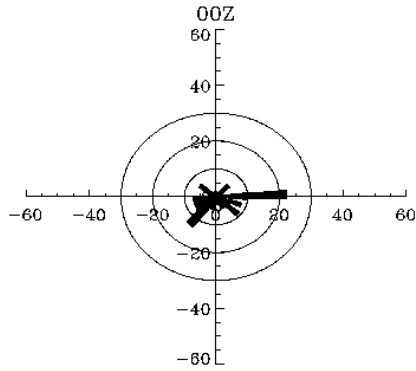
Station Menado (97014) diurnal changes

Station: Mili (6.10N 171.40E)

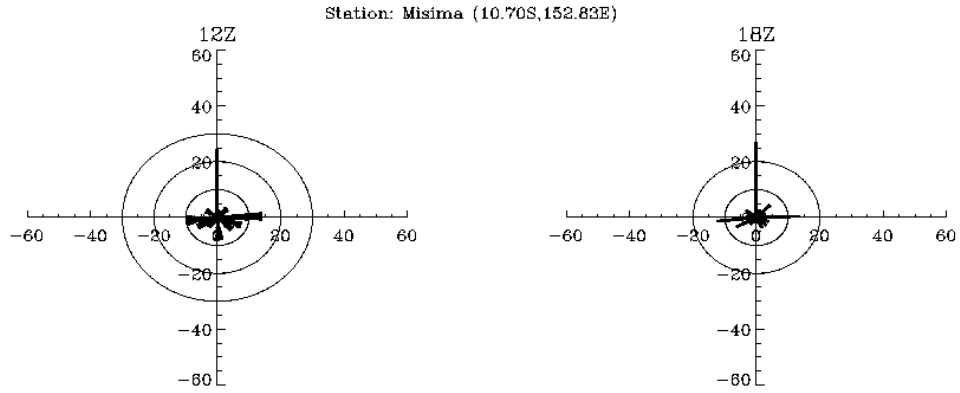


Station Mili (91377) diurnal changes

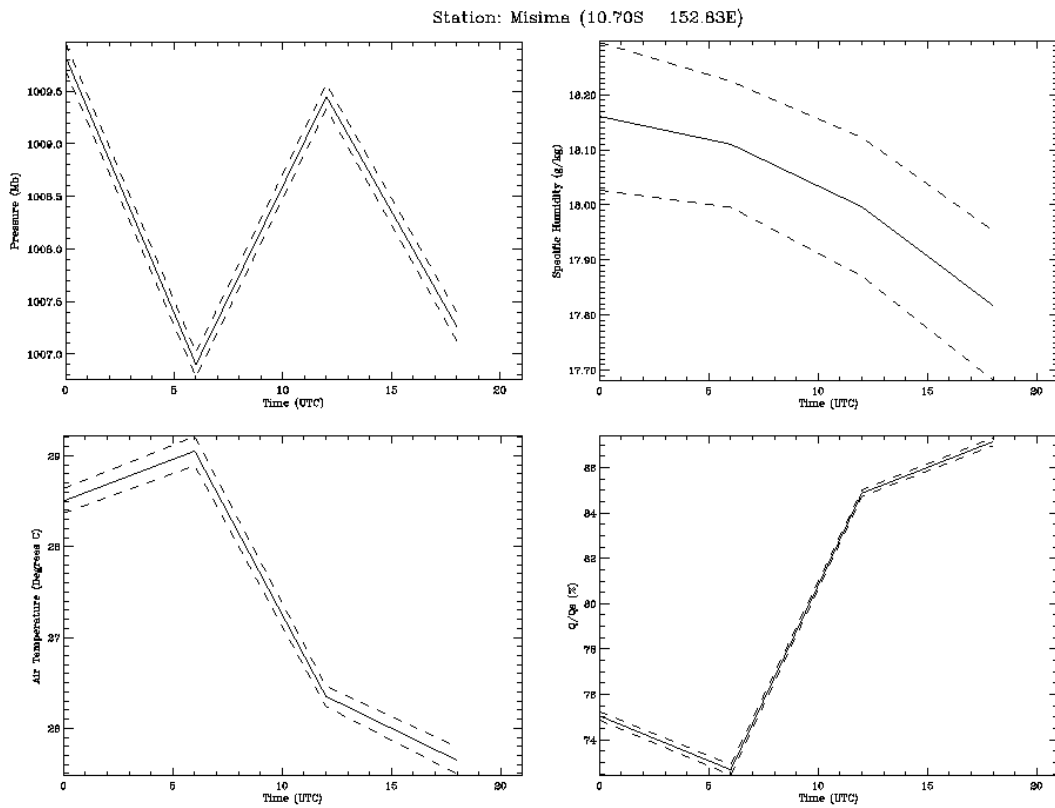
Station: Misima (10.70S,152.82E)



Station Misima (94087) 0,3,6,9 UTC Wind Roses

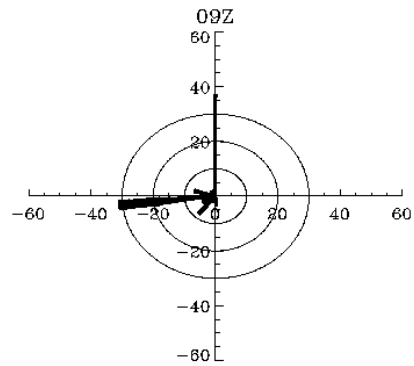
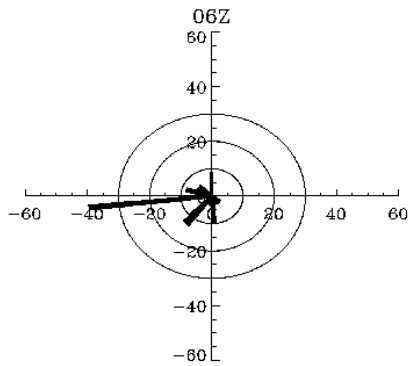
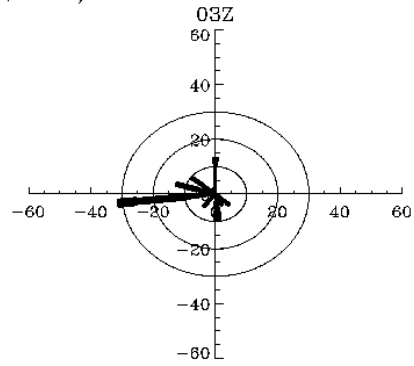
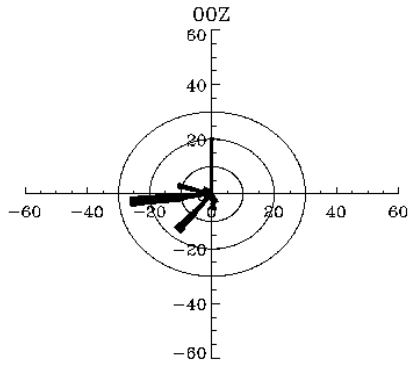


Station Misima (94087) 12,15,18,21 UTC Wind Roses



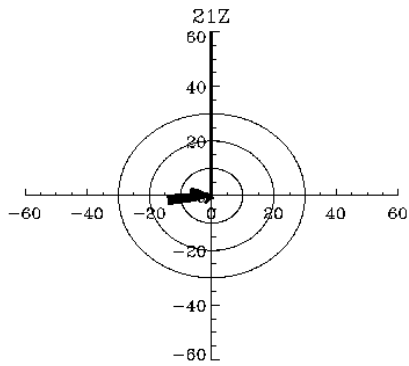
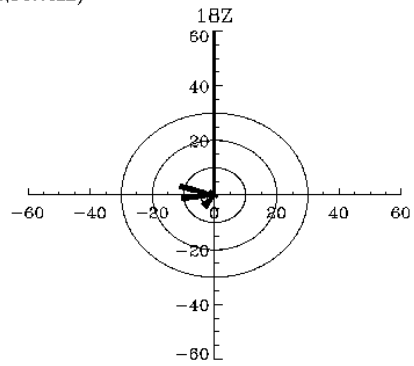
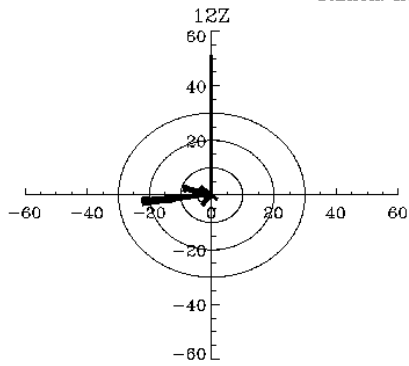
Station Misima (94087) diurnal changes

Station: Momote (2.07S,147.43E)



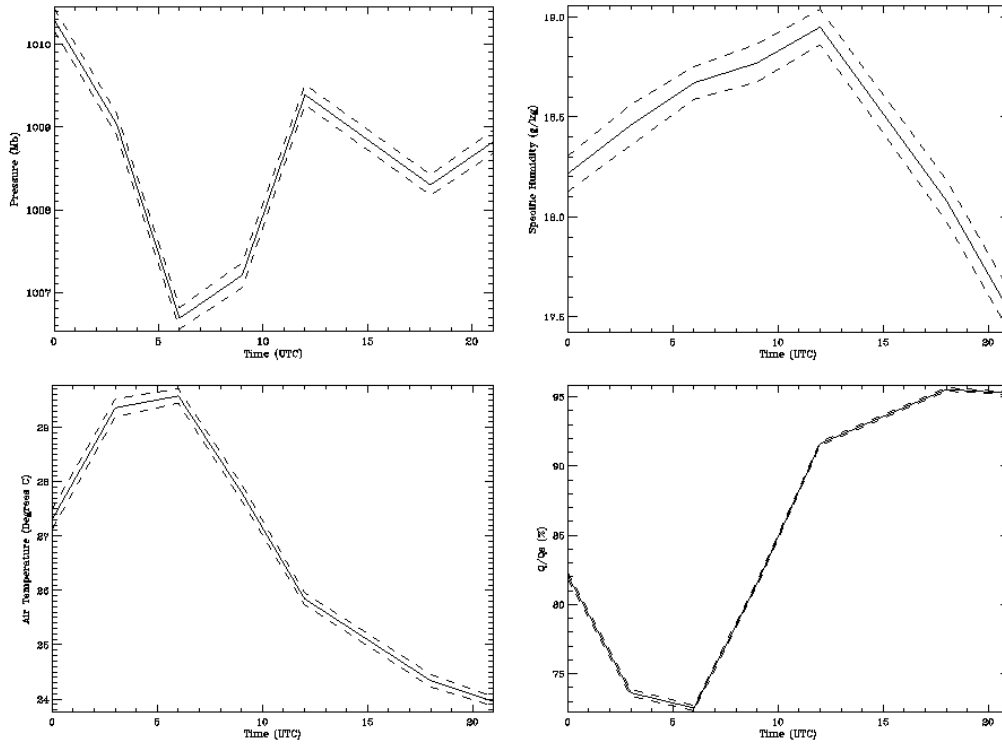
Station Momote (94044) 0,3,6,9 UTC Wind Roses

Station: Momote (2.07S,147.43E)



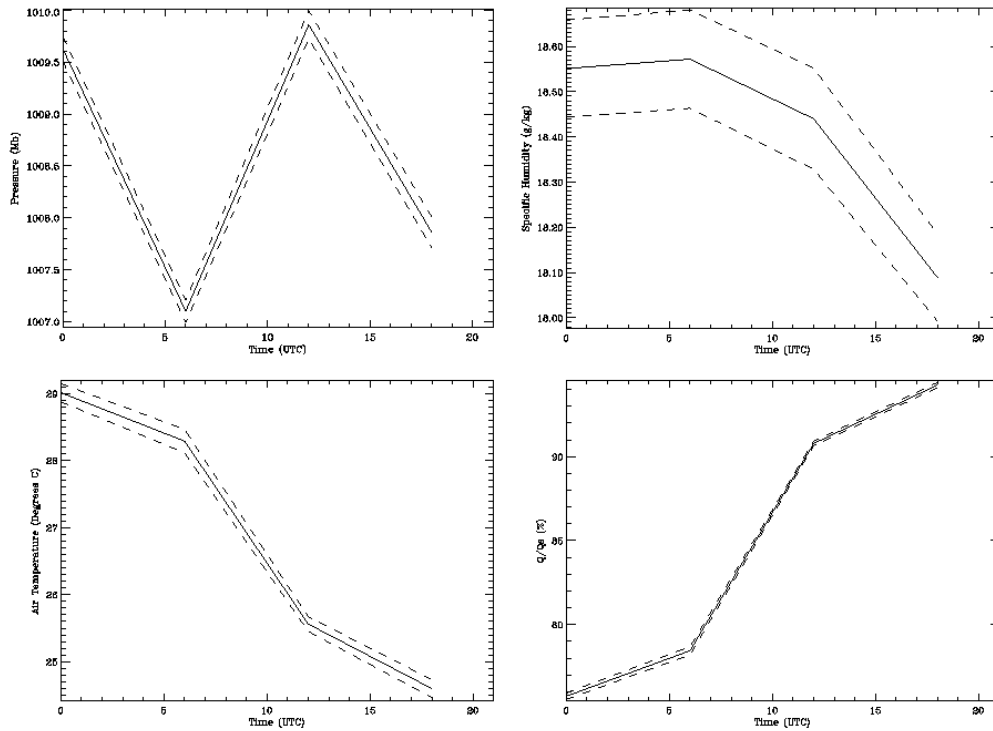
Station Momote (94044) 12,15,18,21 UTC Wind Roses

Station: Momote (2.07S 147.43E)



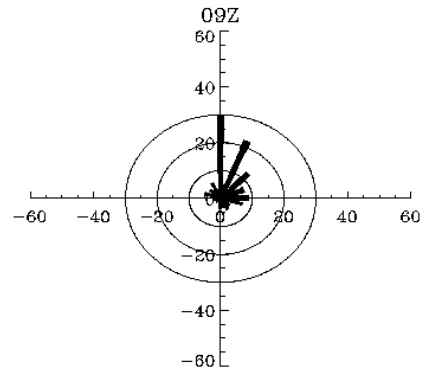
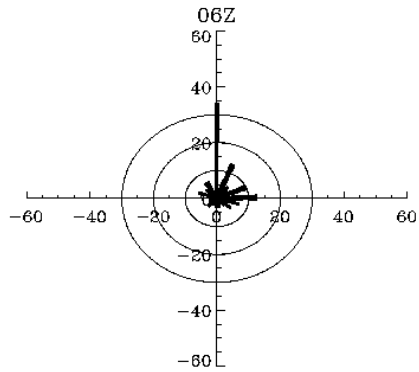
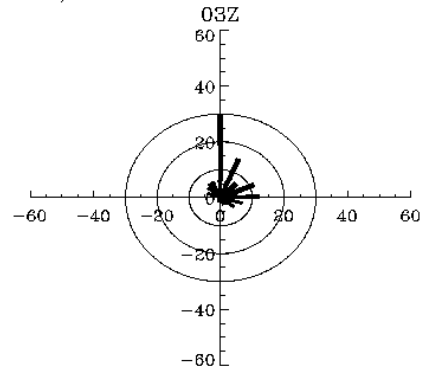
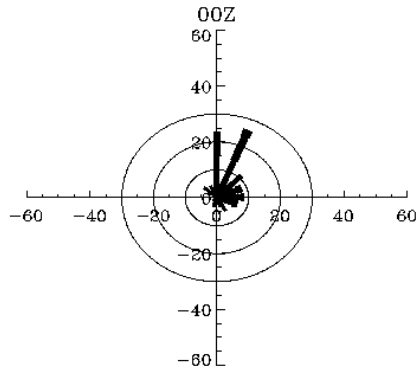
Station Momote (94044) diurnal changes

Station: Munda (8.33S 157.27E)



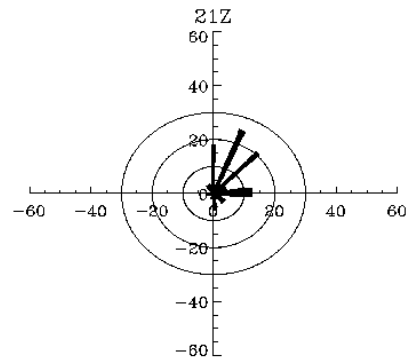
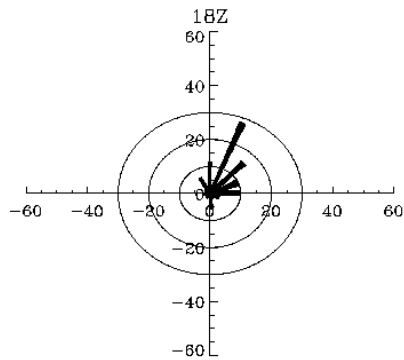
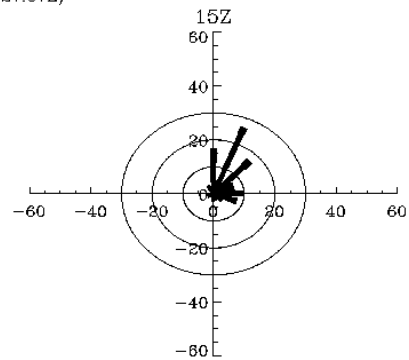
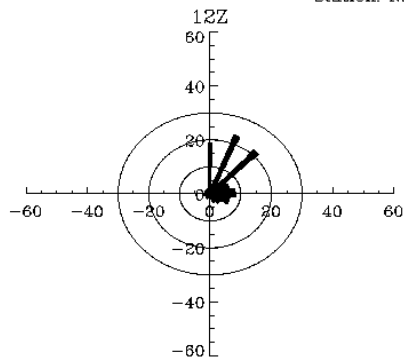
Station Munda (91503) diurnal changes

Station: Naha (26.20N,127.67E)



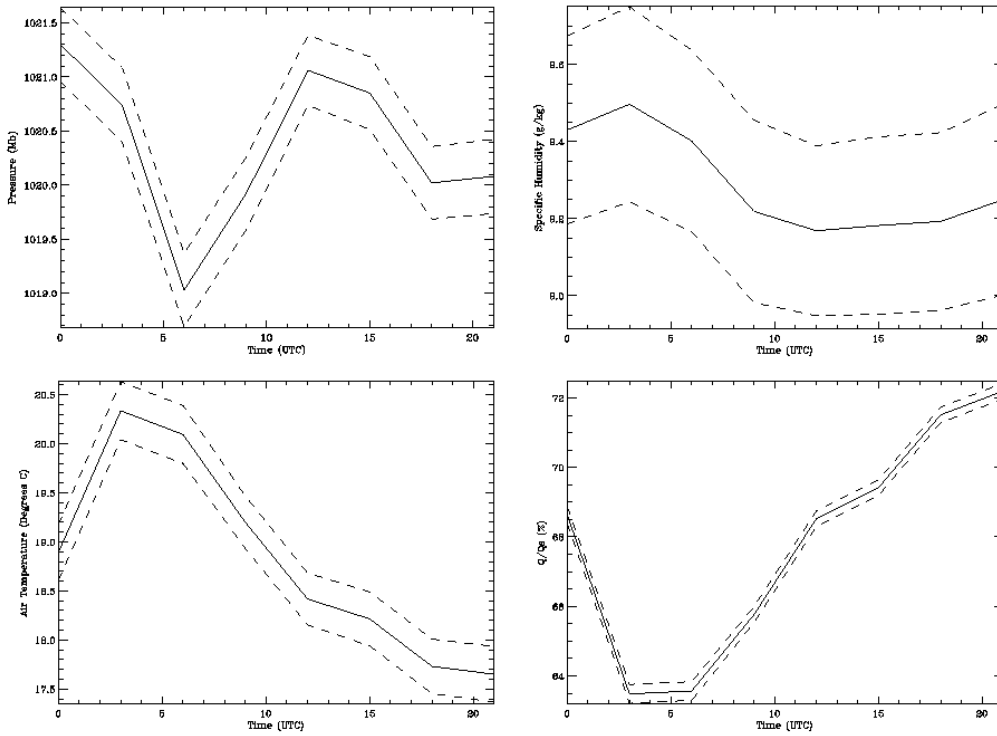
Station Naha (47936) 0,3,6,9 UTC Wind Roses

Station: Naha (26.20N,127.67E)



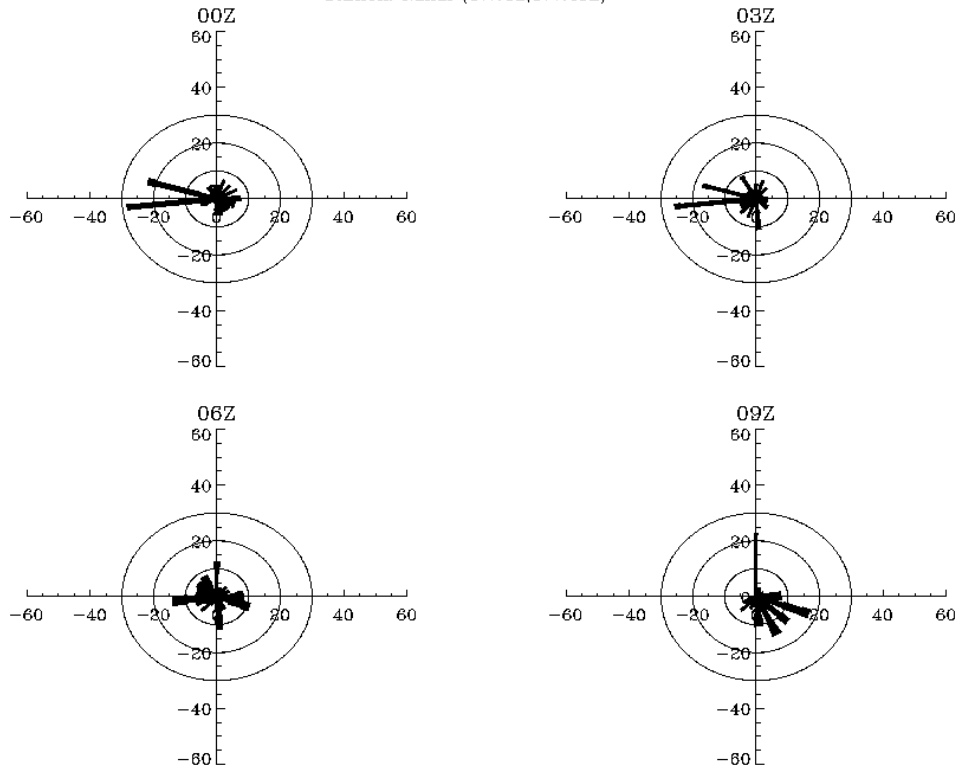
Station Naha (47936) 12,15,18,21 UTC Wind Roses

Station: Naha (26.23N 127.68E)



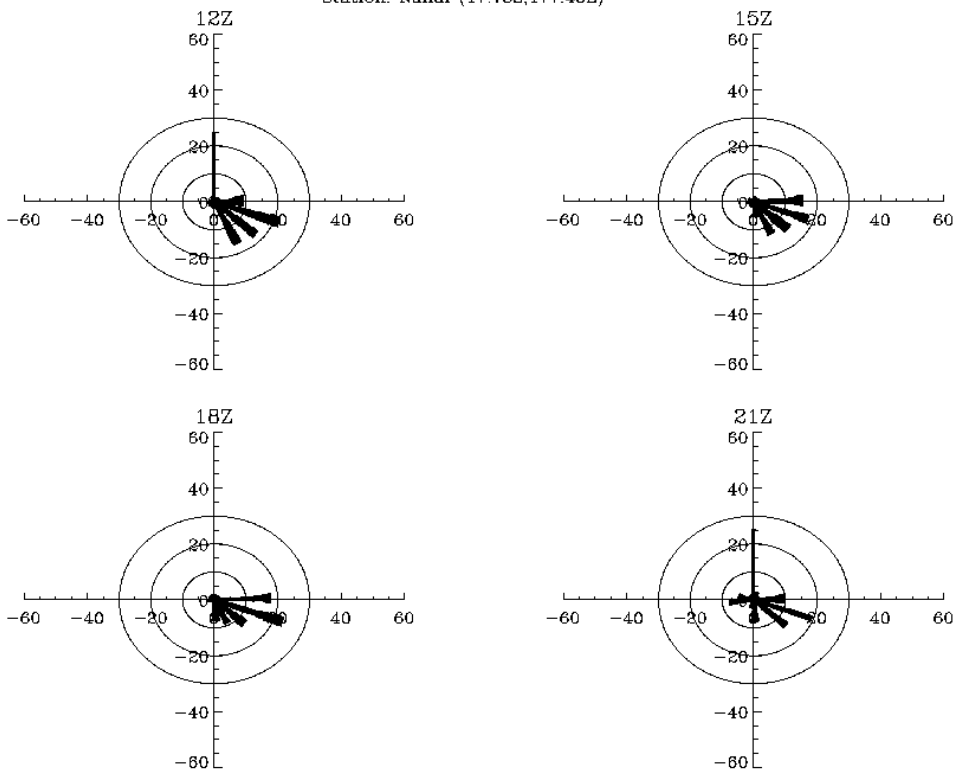
Station Naha (47936) diurnal changes

Station: Nandi (17.75S,177.45E)



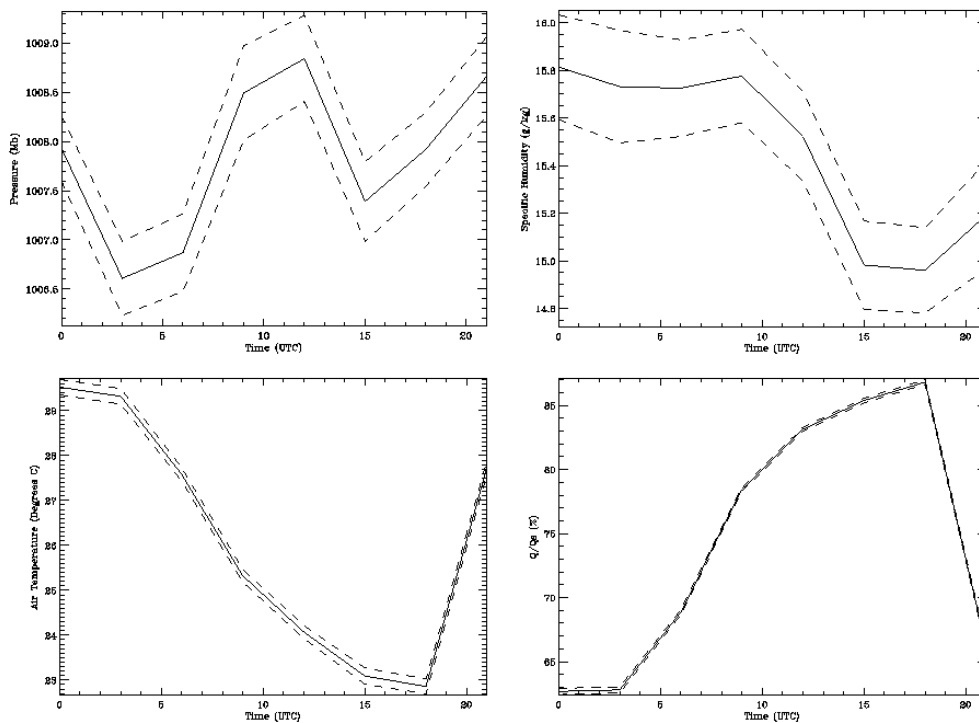
Station Nandi (91680) 0,3,6,9 UTC Wind Roses

Station: Nandi (17.75S,177.45E)



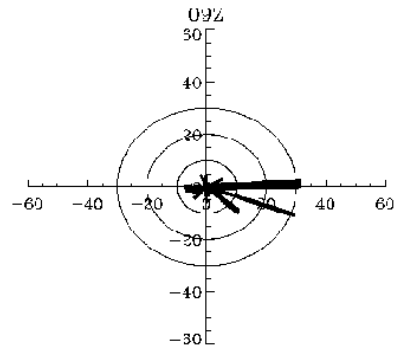
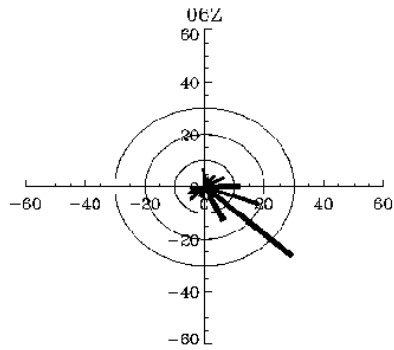
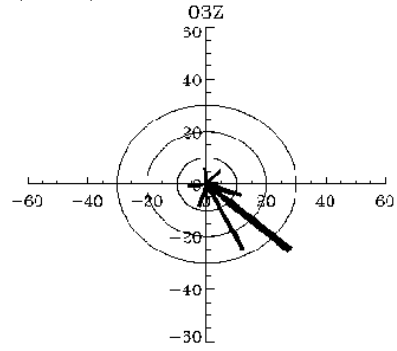
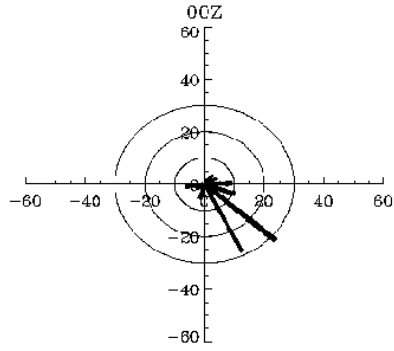
Station Nandi (91680) 12,15,18,21 UTC Wind Roses

Station: Nandi (17.75S 177.45E)



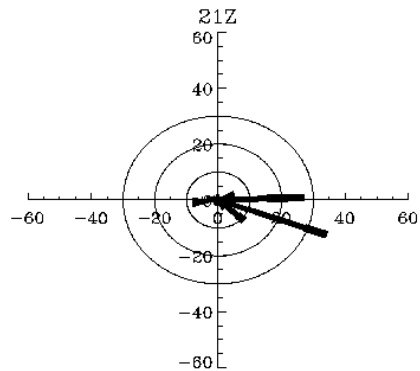
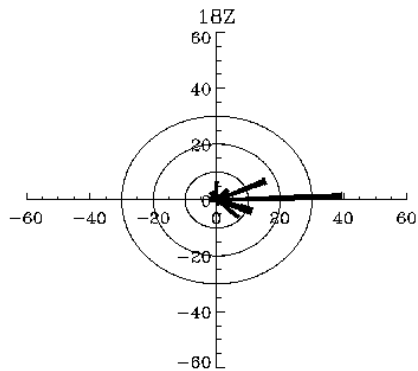
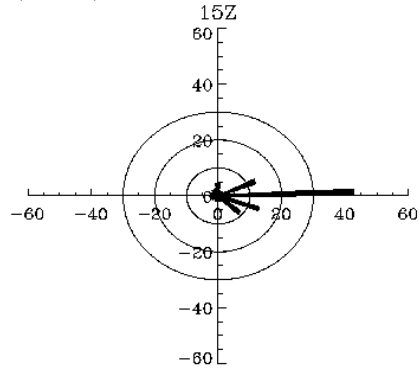
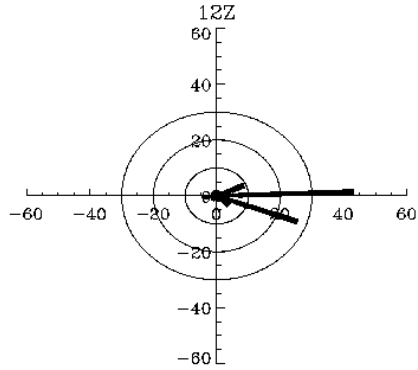
Station Nandi (91680) diurnal changes

Station: Noumeae (22.27S,166.45E)



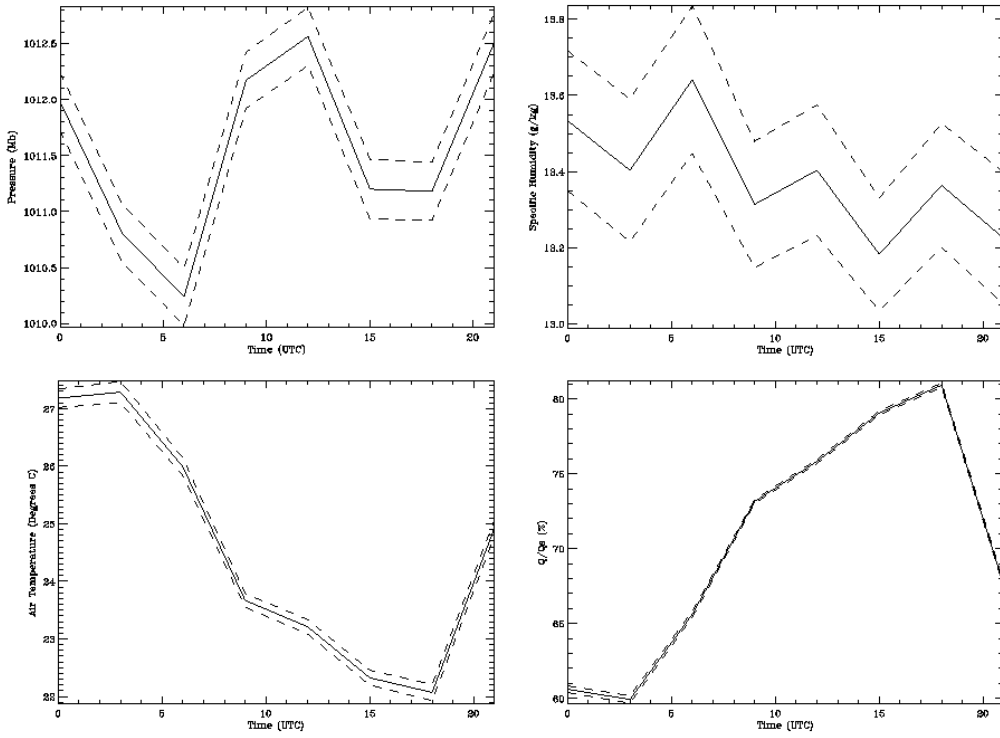
Station Noumea (91592) 0,3,6,9 UTC Wind Roses

Station: Noumeae (22.27S,166.45E)



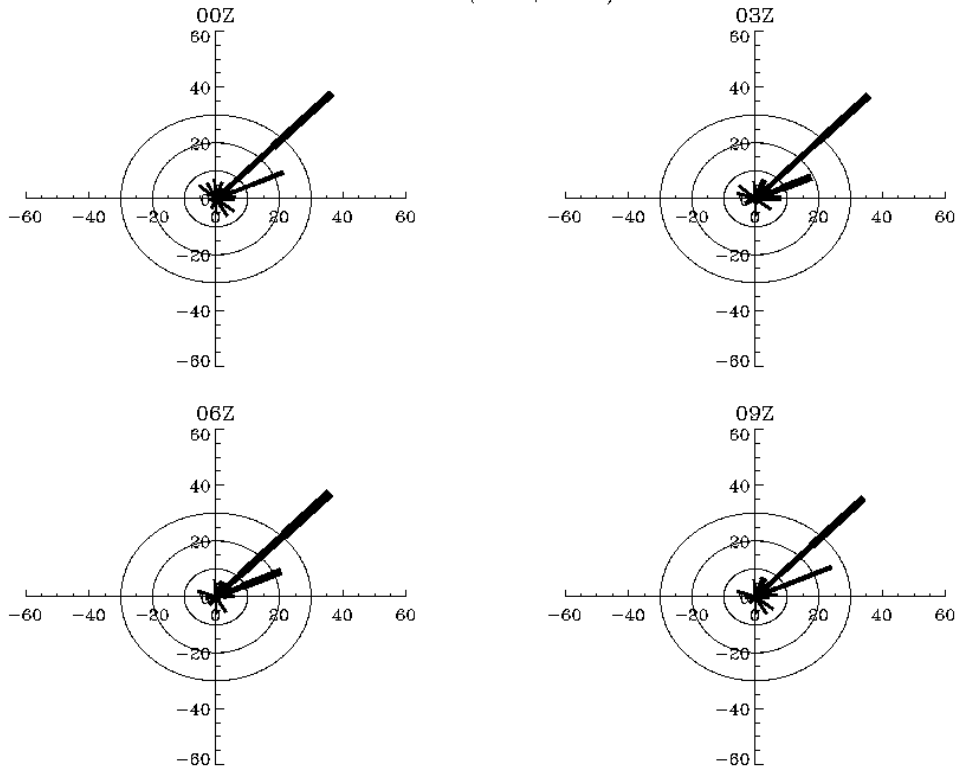
Station Noumea (91592) 12,15,18,21 UTC Wind Roses

Station: Noumea (22.27S 166.45E)



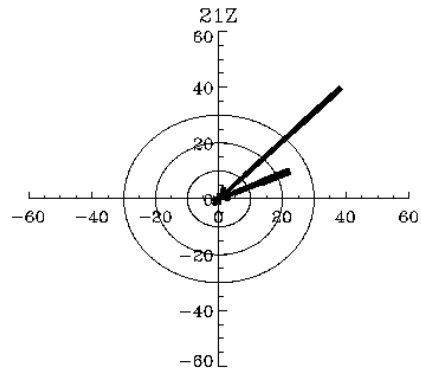
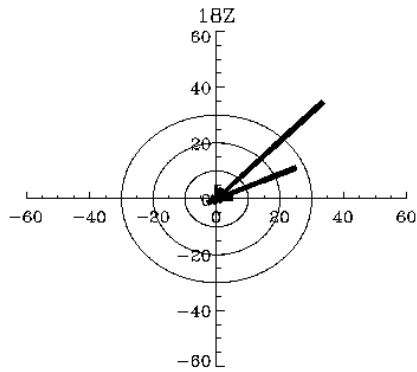
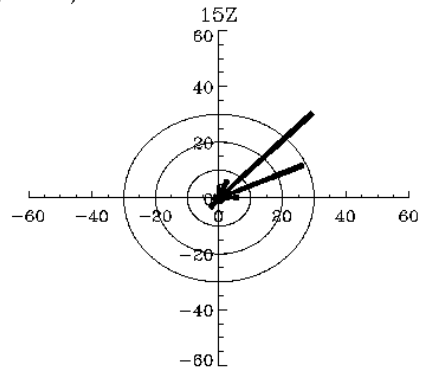
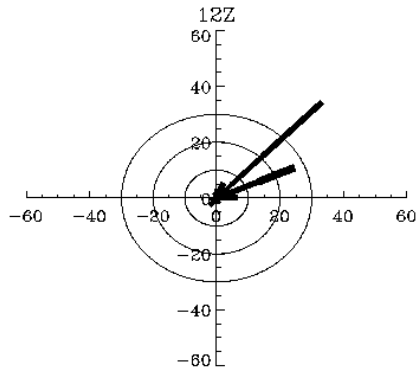
Station Noumea (91592) diurnal changes

Station: Oroluk (7.63N,155.17E)



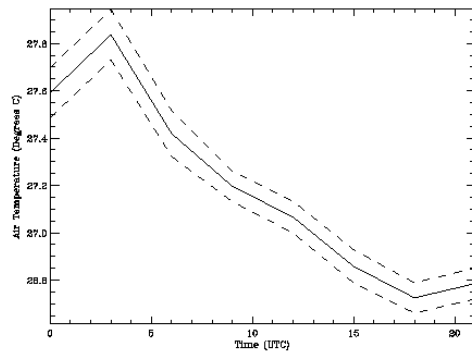
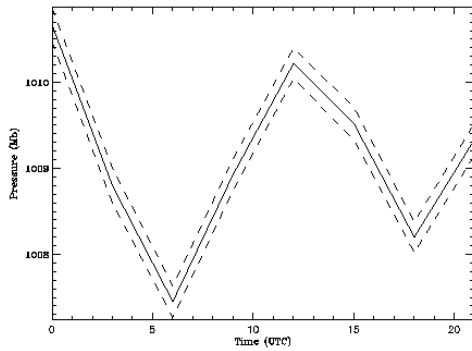
Station Oroluk (91343) 0,3,6,9 UTC Wind Roses

Station: Oroluk (7.63N,155.17E)



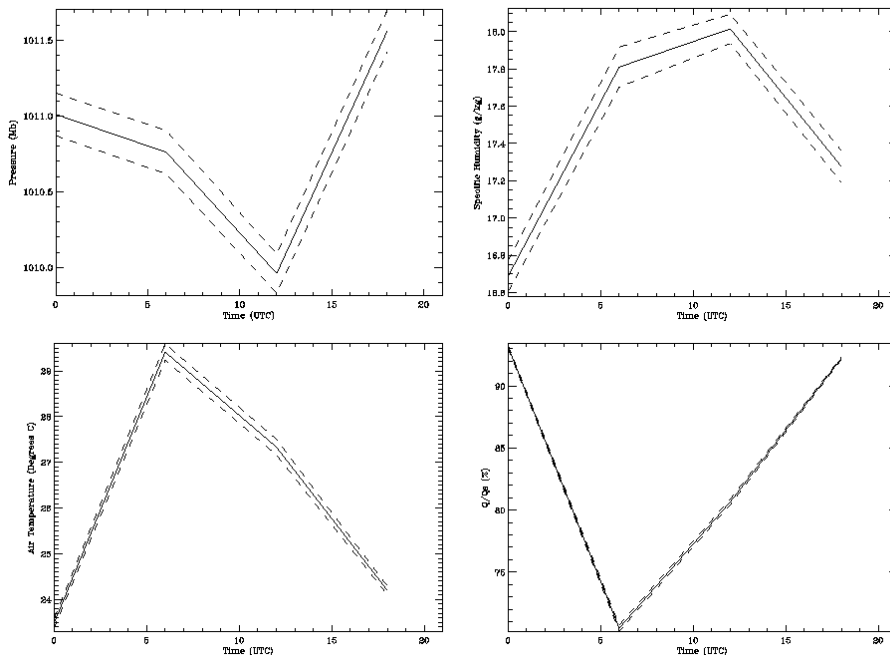
Station Oroluk (91343) 12,15,18,21 UTC Wind Roses

Station: Oroluk (7.63N 155.17E)



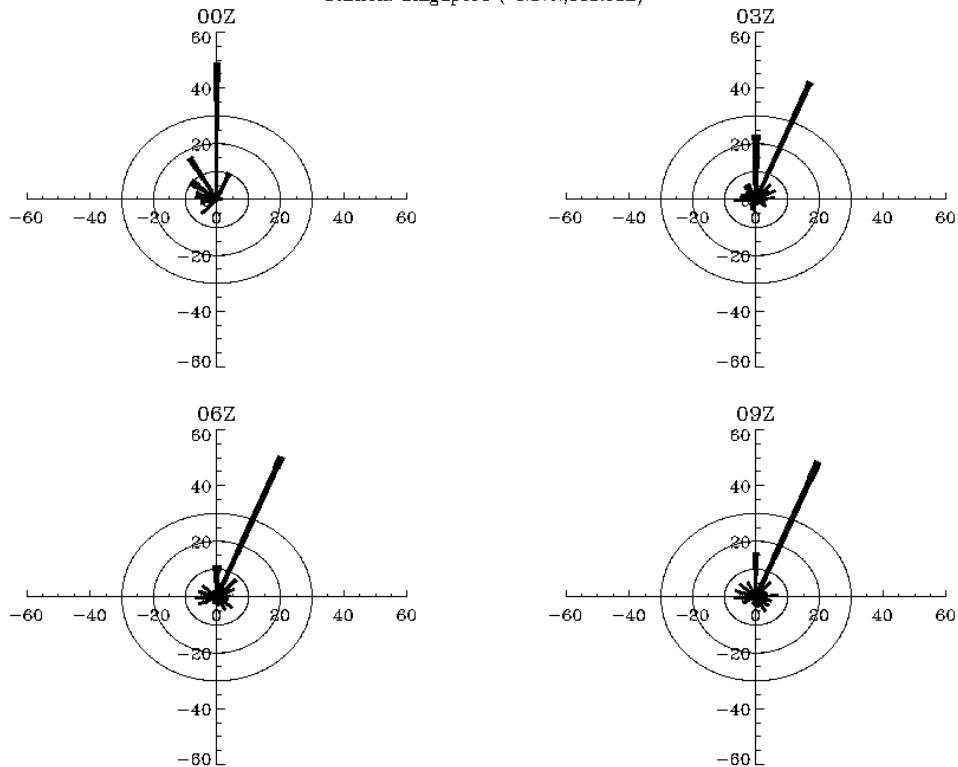
Station Oroluk (91343) diurnal changes

Station: Padang (0.88S 100.35E)

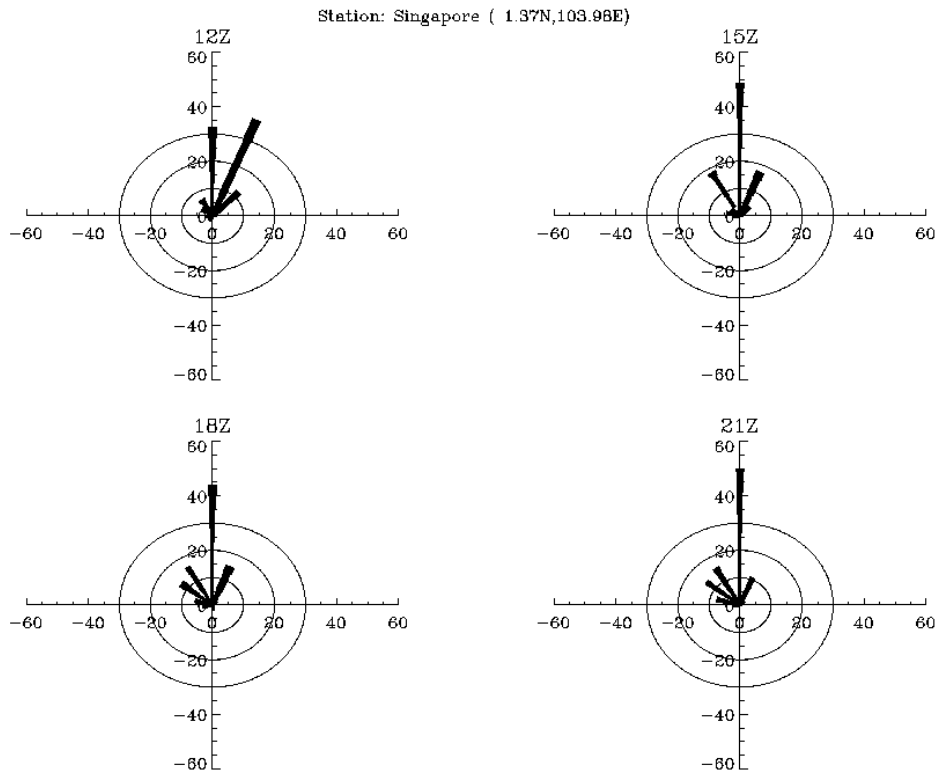


Station Padang diurnal changes

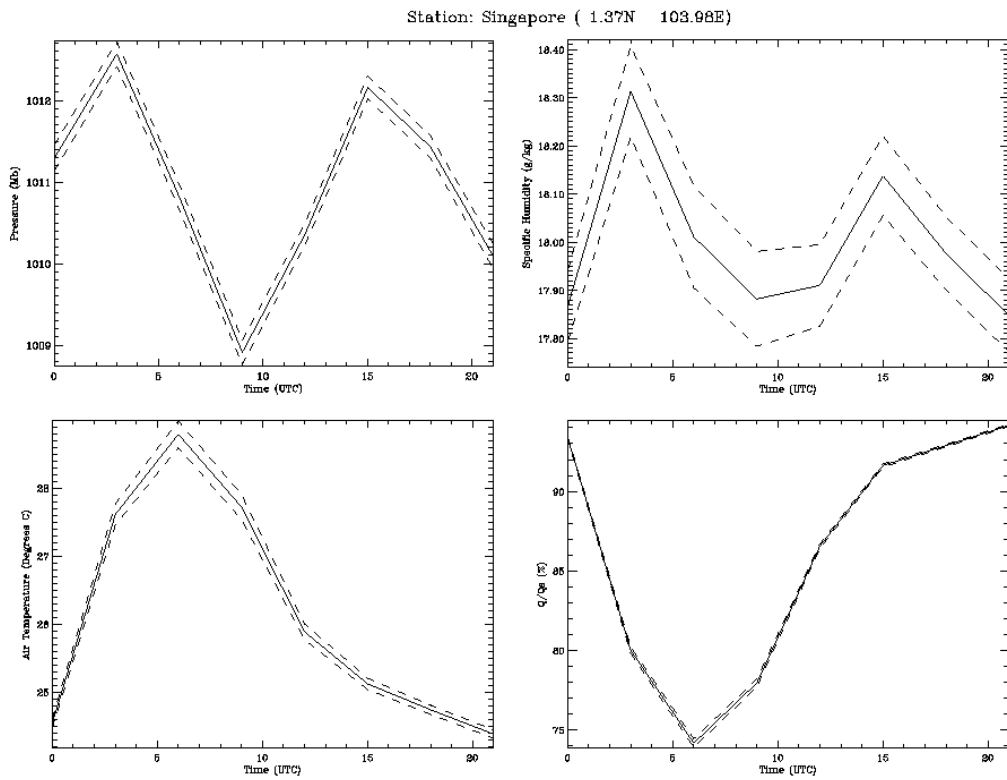
Station: Singapore (1.37N,103.98E)



Station Singapore (48698) 0,3,6,9 UTC Wind Roses

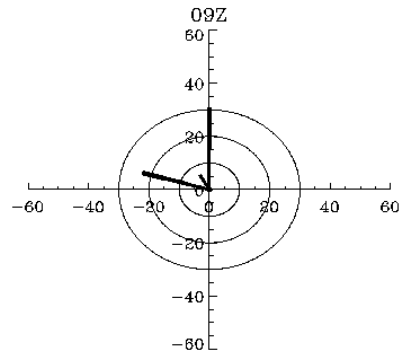
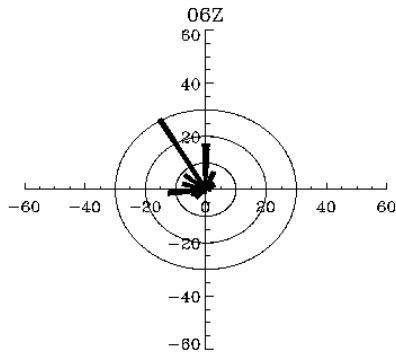
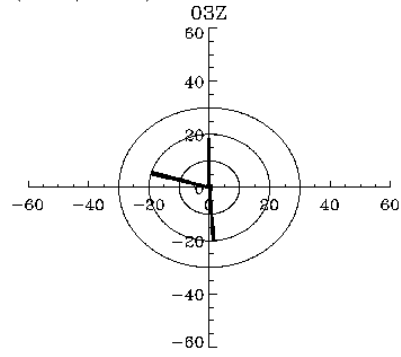
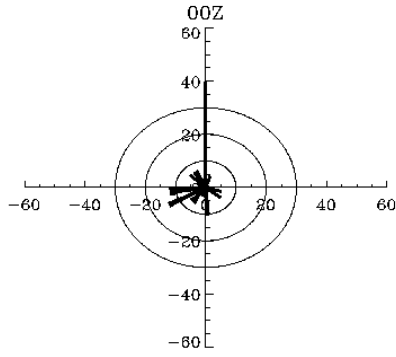


Station Singapore (48698) 12,15,18,21 UTC Wind Roses



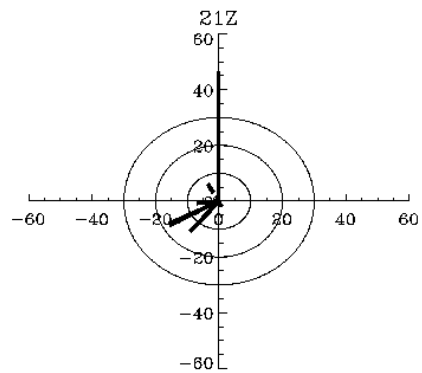
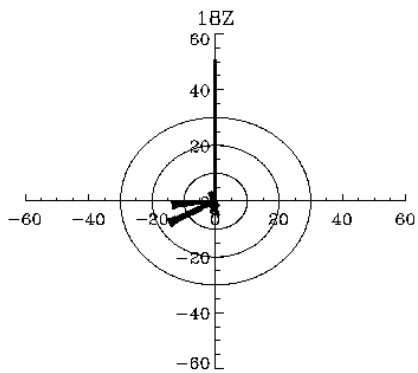
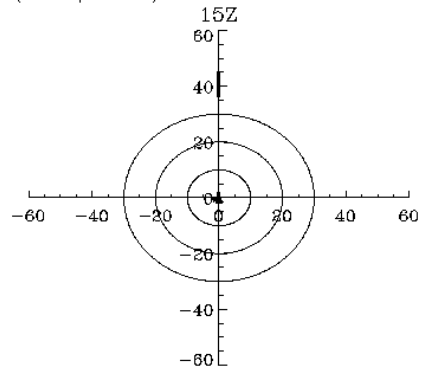
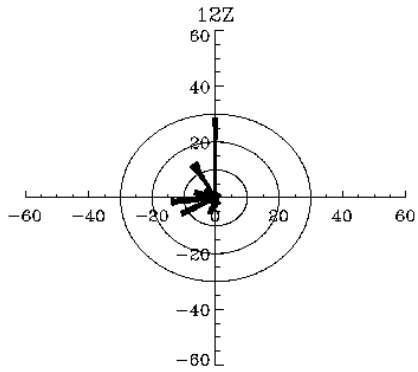
Station Singapore (48698) diurnal changes

Station: Soekarno_Hatta (6.12S,106.65E)



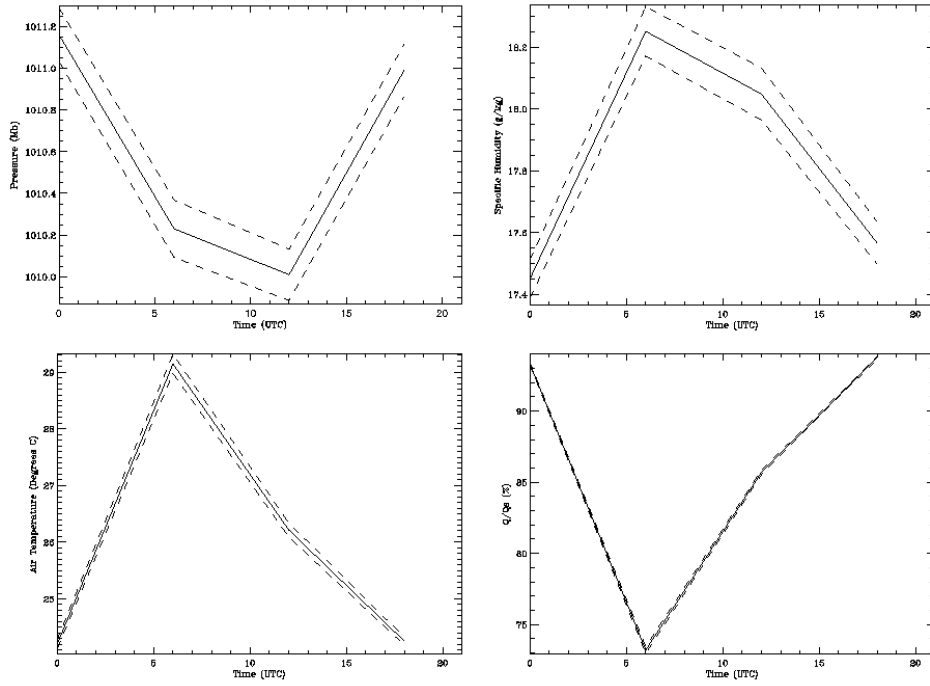
Station Soekarno-Hatta (96749) 0,3,6,9 UTC Wind Roses

Station: Soekarno_Hatta (6.12S,106.65E)



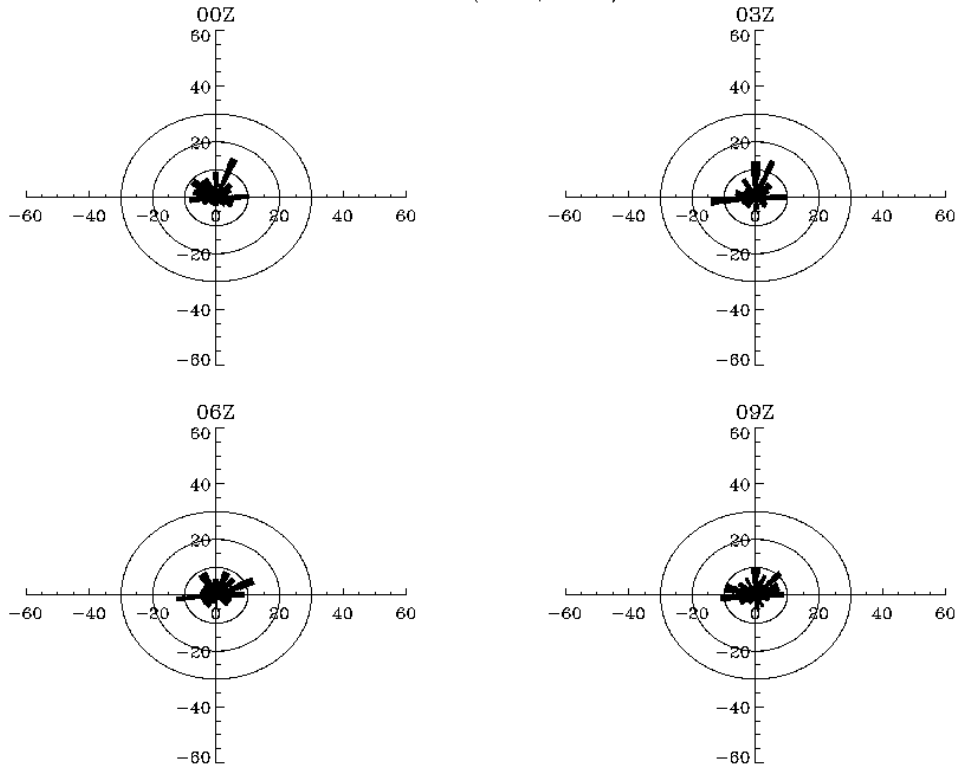
Station Soekarno-Hatta (96749) 12,15,18,21 UTC Wind Roses

Station: Soekarno-Hatta (6.12S 106.65E)



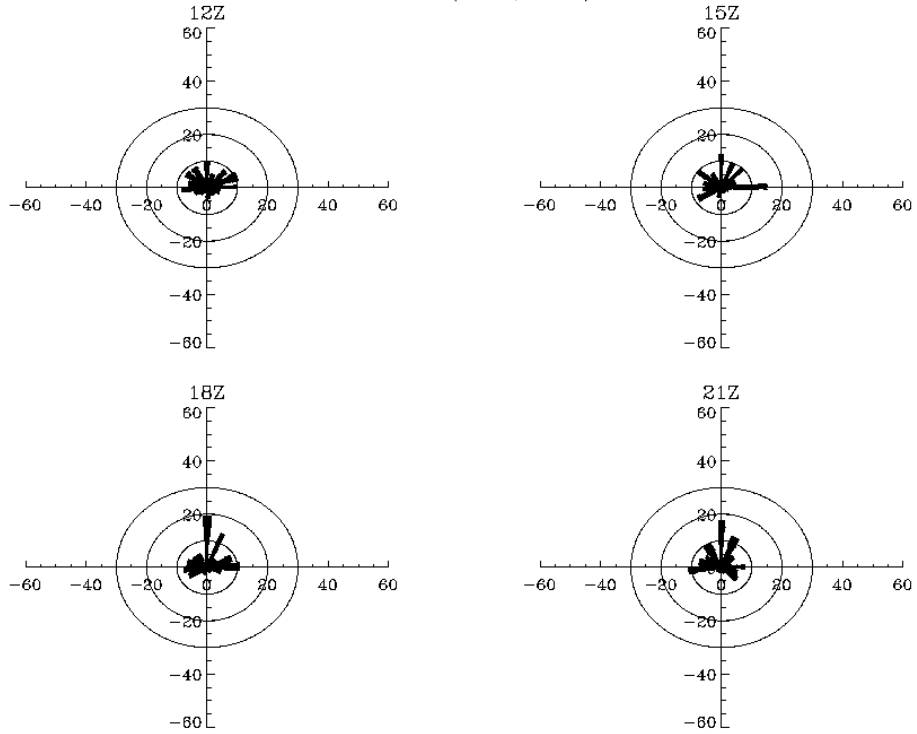
Station Soekarno-Hatta (96749) diurnal changes

Station: Tarawa (1.35N,172.92E)



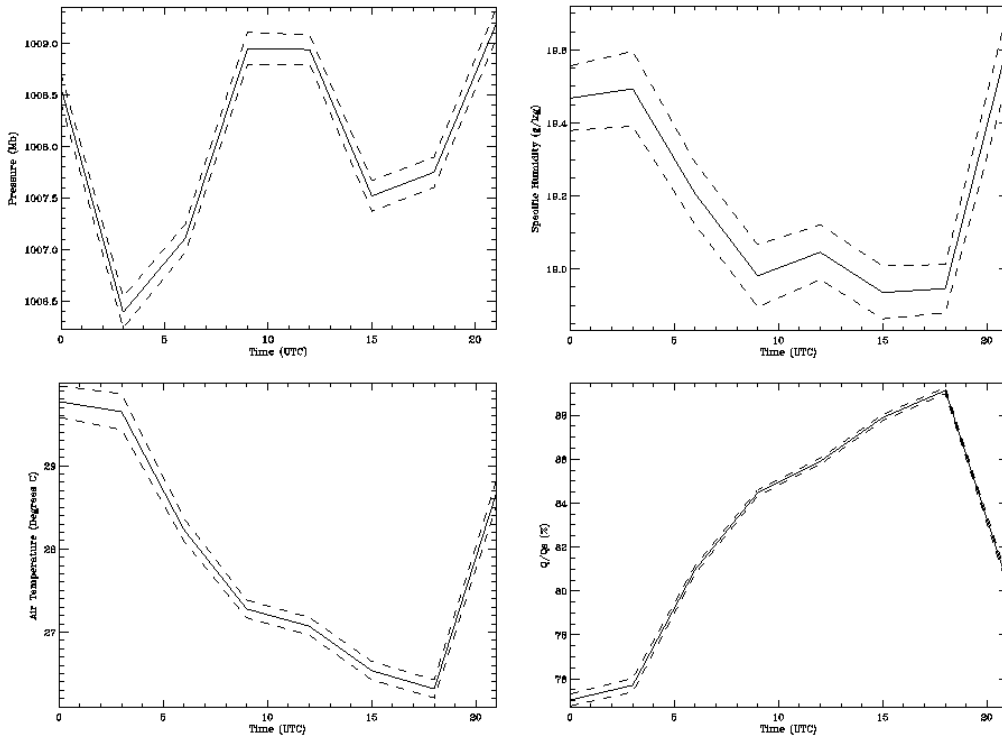
Station Tarawa (91610) 0,3,6,9 UTC Wind Roses

Station: Tarawa (1.35N,172.92E)



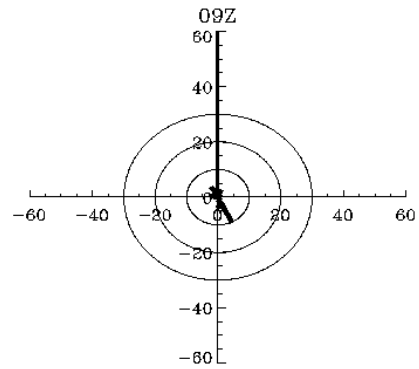
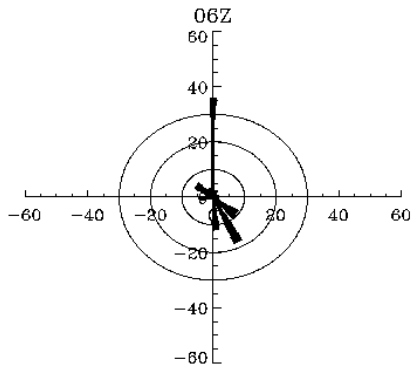
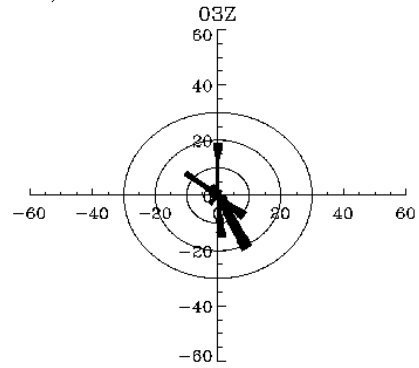
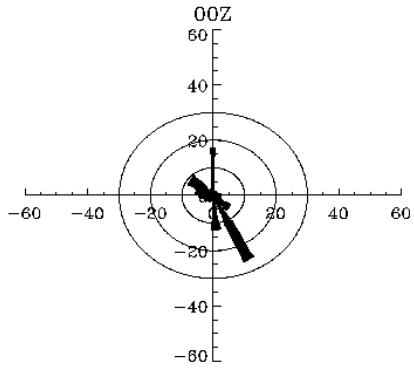
Station Tarawa (91610) 12,15,18,21 UTC Wind Roses

Station: Tarawa (1.35N 172.92E)



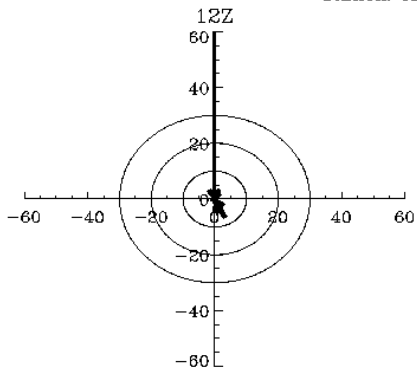
Station Tarawa (91610) diurnal changes

Station: Taro (6.70S,156.38E)



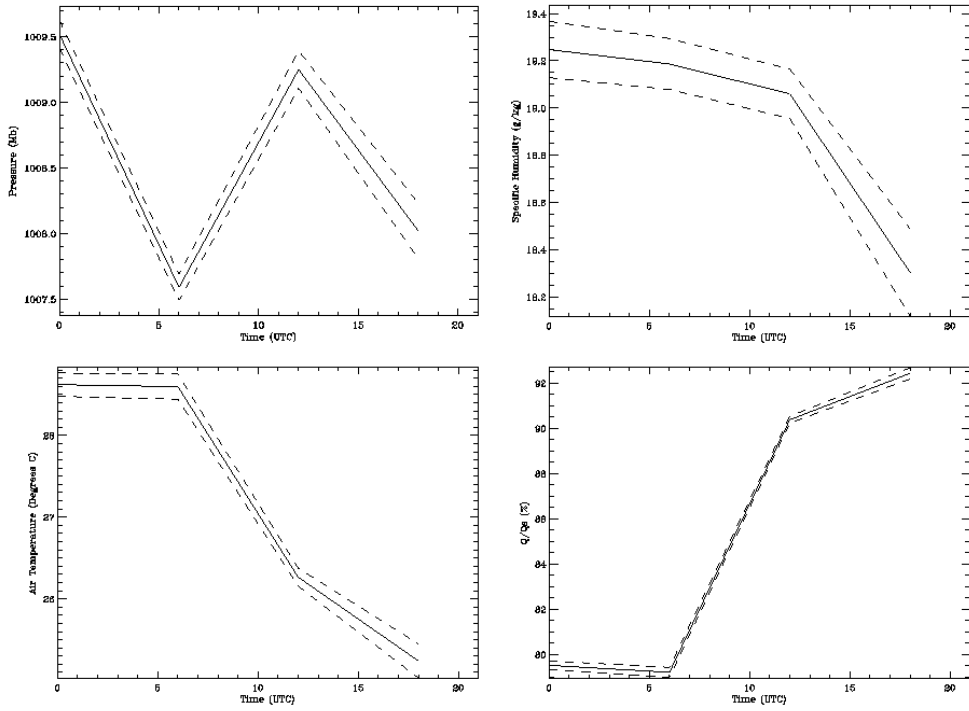
Station Taro (91502) 0,3,6,9 UTC Wind Roses

Station: Taro (6.70S,156.38E)



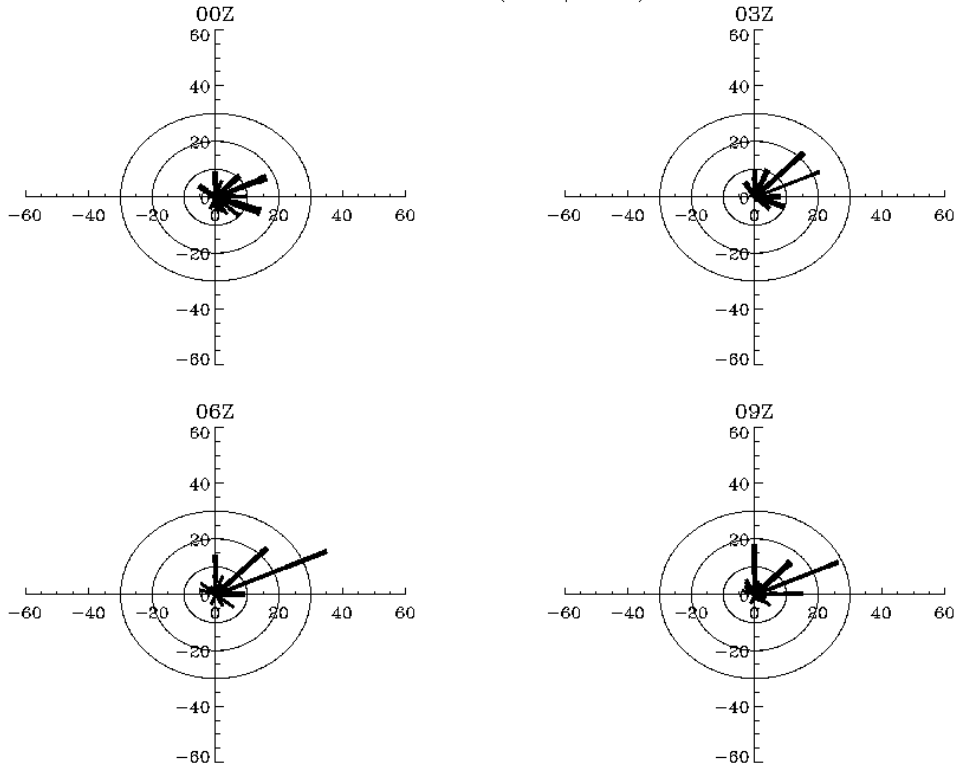
Station Taro (91502) 12,15,18,21 UTC Wind Roses

Station: Taro (6.70S 156.38E)



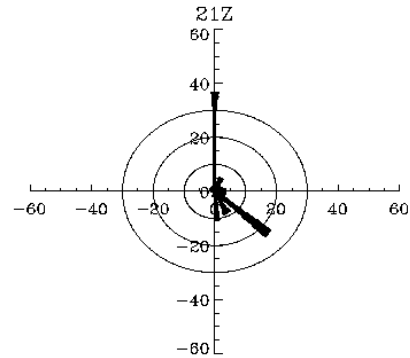
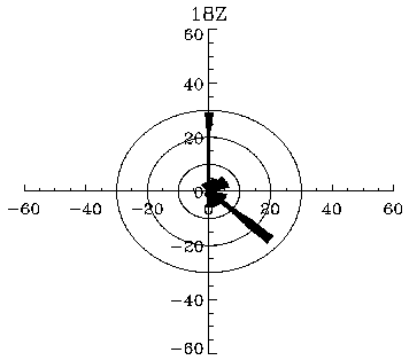
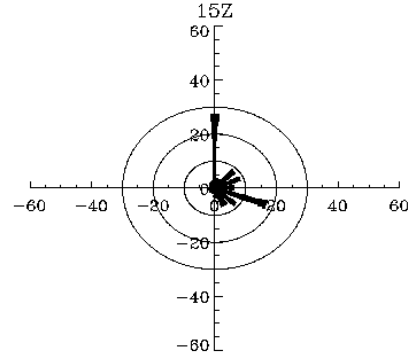
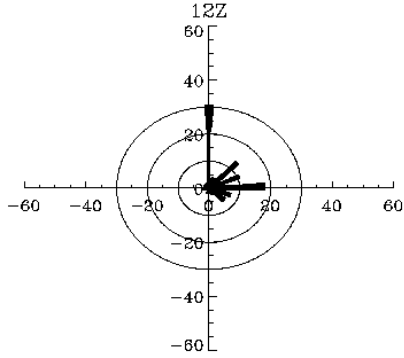
Station Taro (91502) diurnal changes

Station: Townsville (17.75S,177.45E)



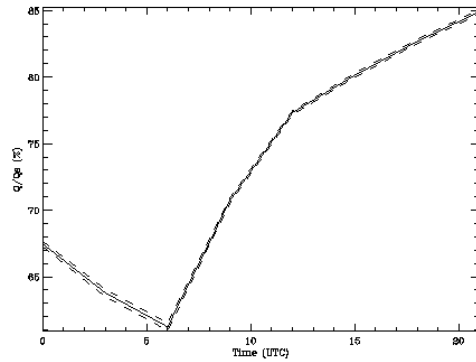
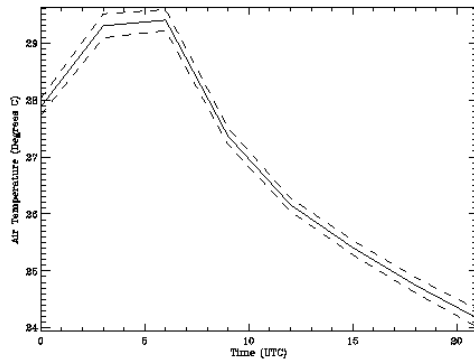
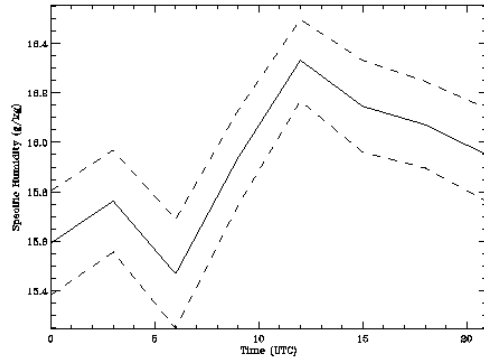
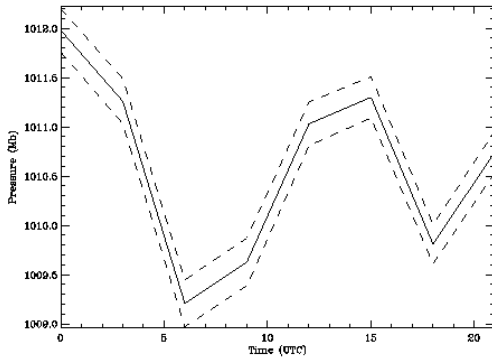
Station Townsville (94294) 0,3,6,9 UTC Wind Roses

Station: Townsville (17.75S,177.45E)



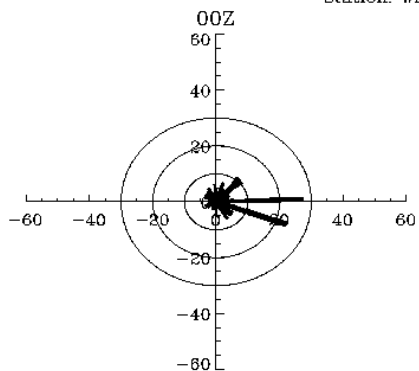
Station Townsville (94294) 12,15,18,21 UTC Wind Roses

Station: Townsville (19.25S 146.77E)



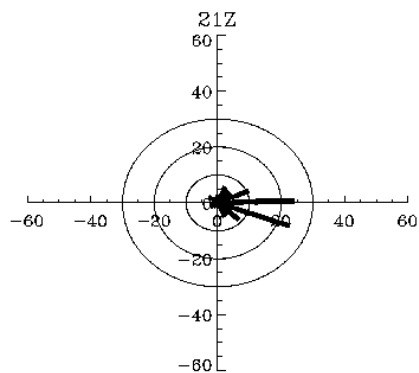
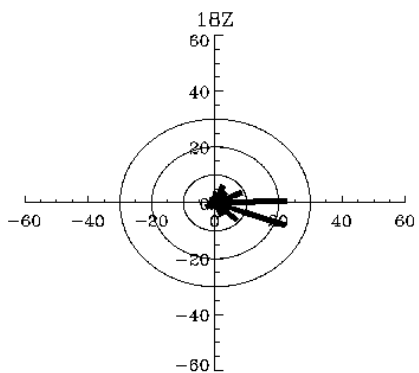
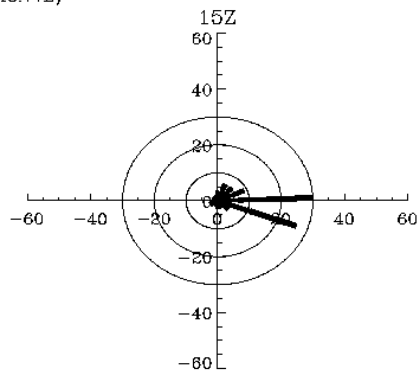
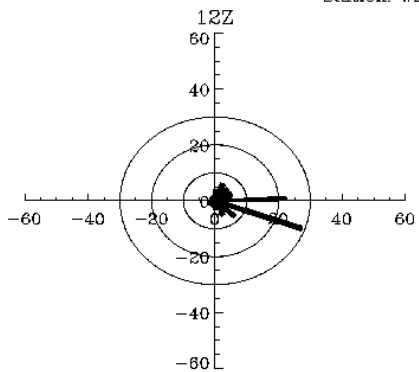
Station Townsville (94294) diurnal changes

Station: Willis (19.25S,146.77E)



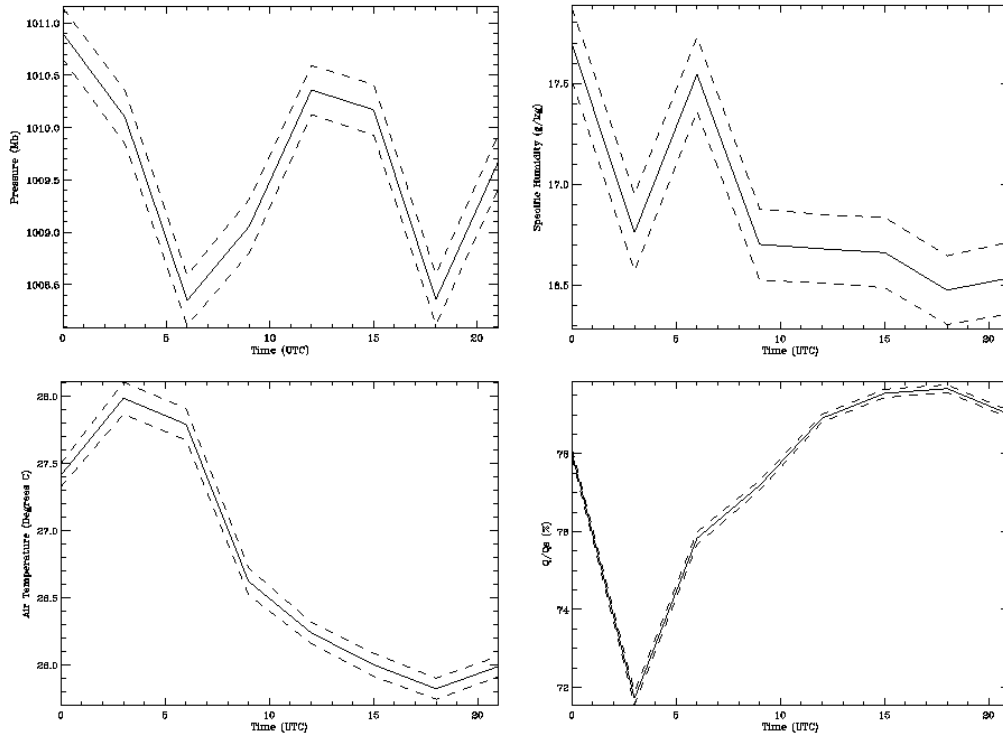
Station Willis (94299) 0,3,6,9 UTC Wind Roses

Station: Willis (19.25S,146.77E)



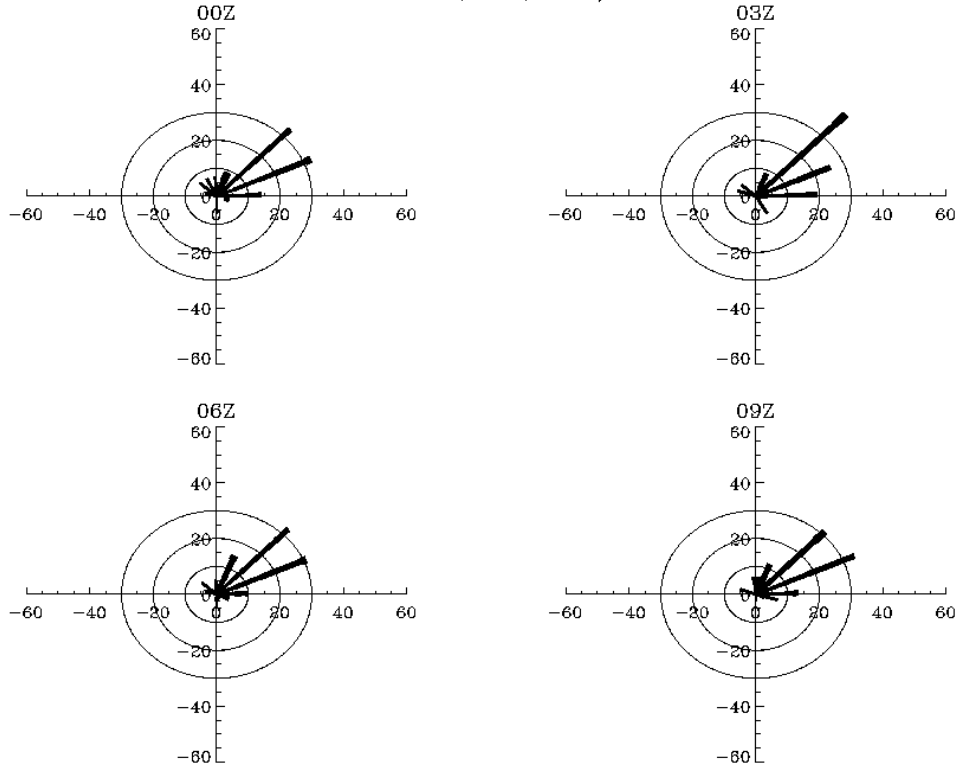
Station Willis (94299) 12,15,18,21 UTC Wind Roses

Station: Willis (16.30S 149.98E)



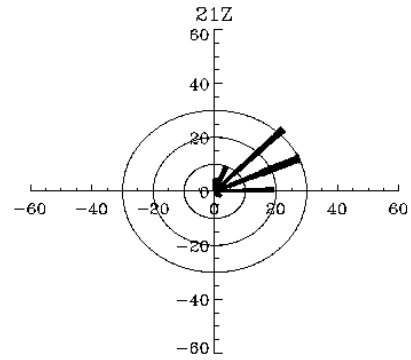
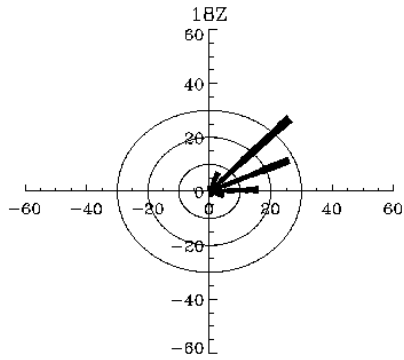
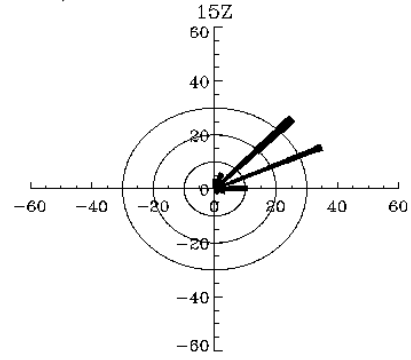
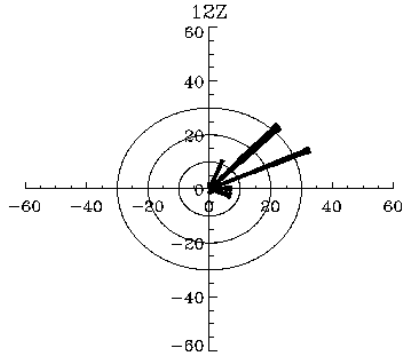
Station Willis (94299) diurnal changes

Station: Xisha (16.83N,112.33E)



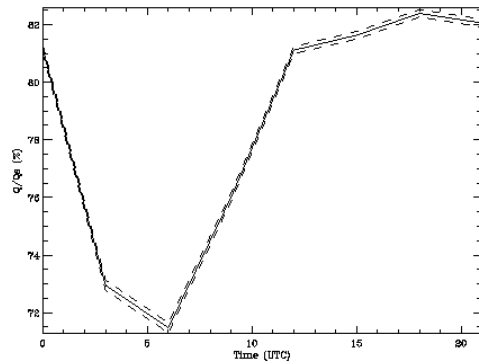
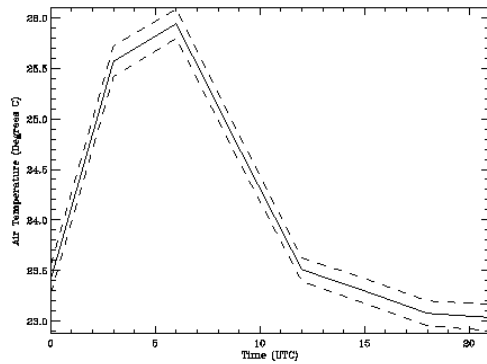
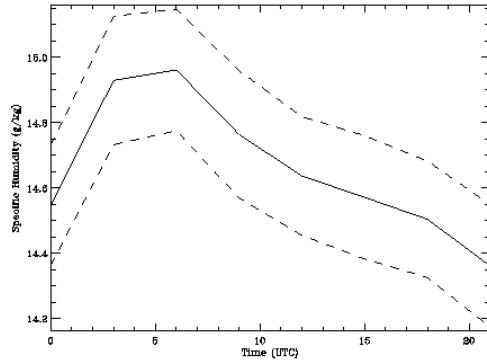
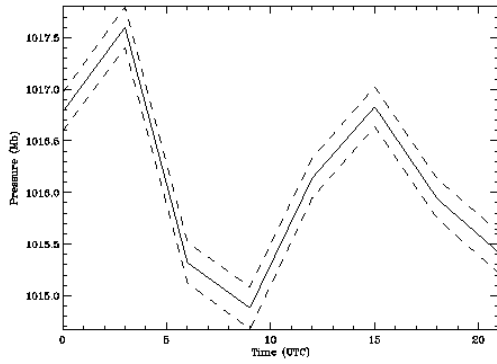
Station Xisha (59981) 0,3,6,9 UTC Wind Roses

Station: Xisha (16.83N,112.33E)



Station Xisha (59981) 12,15,18,21 UTC Wind Roses

Station: Xisha (16.83N 112.33E)



Station Xisha (59981) diurnal changes